The interpretation of temperature and salinity variables in numerical ocean model output, and the calculation of heat fluxes and heat content

by

Trevor J. McDougall[1], Paul M. Barker[1], Ryan M. Holmes[1,2,3], Rich Pawlowicz[4], Stephen M. Griffies[5] and Paul J. Durack[6]

[1]School of Mathematics and Statistics, University of New South Wales, Sydney, NSW 2052, Australia

[2]Climate Change Research Centre and ARC Centre of Excellence for Climate Extremes, University of New South Wales, Sydney, NSW 2052, Australia

[3]Current affiliation: School of Geosciences, University of Sydney, Sydney, NSW 2006, Australia

[4]Dept. of Earth and Ocean Sciences, University of British Columbia, Vancouver, B.C. V6T 1Z4, Canada

[5]NOAA/Geophysical Fluid Dynamics Laboratory, and Princeton University Atmospheric and Oceanic Sciences Program, Princeton, New Jersey, USA

[6]Program for Climate Model Diagnosis and Intercomparison, Lawrence Livermore National Laboratory, Livermore, California, USA

Corresponding author email: Trevor.McDougall@unsw.edu.au

Full address
Trevor J McDougall
School of Mathematics and Statistics
University of New South Wales, NSW 2052, Australia
tel: +61 2 9385 3498
fax: +61 2 9385 7123
mob: +61 407 518 183

keywords ocean modelling, CMIP, ocean model intercomparison, TEOS-10, EOS-80,

Submitted to *Geoscientific Model Development*

This version is dated 30th September 2021

Abstract

The international thermodynamic equation of seawater of 2010 (TEOS-10) defined the enthalpy and entropy of seawater, thus enabling the global ocean heat content to be calculated as the volume integral of the product of in situ density, ρ, and potential enthalpy, h^0 (with reference sea pressure of 0 dbar). In terms of Conservative Temperature, Θ, ocean heat content is the volume integral of $\rho c_p^0 \Theta$, where c_p^0 is a constant "isobaric heat capacity".

However, many ocean models in the Coupled Model Intercomparison Project phase 6 (CMIP6) as well as all models that contributed to earlier phases, such as CMIP5, CMIP3, CMIP2 and CMIP1 used EOS-80 (Equation of State - 1980) rather than the updated TEOS-10, so the question arises of how the salinity and temperature variables in these models should be physically interpreted, with a particular focus on comparison to TEOS-10 compliant observations. In this article we address how heat content, surface heat fluxes and the meridional heat transport are best calculated using output from these models, and how these quantities should be compared with those calculated from corresponding observations. We conclude that even though a model uses the EOS-80 equation of state which expects potential temperature as its input temperature, the most appropriate interpretation of the model's temperature variable is actually Conservative Temperature. This perhaps unexpected interpretation is needed to ensure that the air-sea heat flux that leaves/arrives-in the atmosphere and sea ice models is the same as that which arrives-in/leaves the ocean model.

We also show that the salinity variable carried by present TEOS-10 based models is Preformed Salinity, while the salinity variable of EOS-80 based models is also proportional to Preformed Salinity. These interpretations of the salinity and temperature variables in ocean models are an update on the comprehensive Griffies et al (2016) paper that discusses the interpretation of many aspects of coupled Earth system models.

1. Introduction

Numerical ocean models simulate the ocean by calculating the acceleration of fluid parcels in response to various forces, some of which are related to spatially-varying density fields that affect pressure, as well as solving transport equations for the two tracers on which density depends, namely temperature [the CMIP6 variables identified as thetao or bigthetao]) and dissolved matter ("salinity", [CMIP6 variable so]). For computational reasons it is useful for the numerical schemes involved to be conservative, meaning that the amount of heat and salt in the ocean changes only due to the area integrated fluxes of heat and salt that cross the ocean's boundaries; in the case of salt, this is zero. This conservative property is guaranteed for ocean models to within computational truncation error since these numerical models are designed using finite volume integrated tracer conservation (e.g., see Appendix F in Griffies et al 2016). It is only by ensuring such conservation properties that scientists can reliably make use of numerical ocean models for the long (centuries and longer) simulations required for climate and Earth system studies.

However, this apparent numerical success ignores some difficult theoretical issues with the equation set being numerically solved. Here, we are concerned with issues related to the properties of seawater that have only recently been widely recognized because of research resulting in the Thermodynamic Equation of Seawater 2010 (TEOS-10). These issues mean that the intercomparison of different models, and comparison with ocean observations, needs to be undertaken with care.

In particular, it is widely recognized that the traditional measure of heat content per unit mass in the ocean (with respect to an arbitrary reference state), the so-called potential temperature, is not a conservative variable (McDougall, 2003). Hence, the time change of potential temperature at a point in space is not determined solely by the convergence of the potential temperature flux at that point. Furthermore, the non-conservative nature of potential temperature means that the potential temperature of a mixture of water masses is not the mass average of the initial potential temperatures since potential temperature is "produced" or "destroyed" by mixing within the ocean's interior. This empirical fact is an inherent property of seawater (e.g., McDougall 2003,

Graham and McDougall 2013), and so treating potential temperature as a conservative tracer (as well as making certain other assumptions related to the modelling of heat and salt) results in contradictions, which have been built into most numerical ocean models to varying degrees.

These contradictions have existed since the beginning of numerical ocean modelling but have generally been ignored or overlooked because many other oceanographic and numerical factors were of greater concern. However, as global heat budgets and their imbalances are now a critical factor in understanding climate changes, it is important to examine the consequences of these assumptions, and perhaps correct them even at the cost of introducing problems elsewhere. These concerns are particularly important when heat budgets are being compared between different models, and with similar calculations made with observed conditions in the real ocean.

The purpose of this paper is to describe these theoretical difficulties, to estimate the magnitude of errors that result, and to make recommendations about resolving them both in current and future modelling efforts. For example, the insistence that a model's temperature variable is potential temperature involves errors in the air-sea heat flux in some areas that are as large as the mean rate of current global warming. A simple re-interpretation of the model's temperature variable overcomes this inconsistency and allows coupled climate models to conserve heat.

The reader who wants to skip straight to the recommendations on how the salinity and temperature outputs of CMIP models should be interpreted can go straight to section 6.

2. Background

Thermodynamic measures of heat content

It is well-known that *in situ* temperature is not a satisfactory measure of the "heat content" of a water parcel because the *in situ* temperature of a water parcel changes as the ambient pressure changes (i.e., if a water parcel is transported to a different depth [pressure] in the ocean). This change is of order 0.1°C as pressure changes 1000 dbar, and is large relative to the precision of 0.01°C required to understand deep ocean

circulation patterns. The utility of *in situ* temperature lies in the fact that it is easily measured with a thermometer, and that air-sea boundary heat fluxes are to some degree proportional to *in situ* temperature differences.

Traditionally, potential temperature has been used as an improved measure of ocean heat content. Potential temperature is defined as the temperature that a parcel would have if moved isentropically and without exchange of mass to a fixed reference pressure (usually taken to be surface atmospheric pressure), and can be calculated from measured ocean *in situ* temperatures using empirical correlation equations based on laboratory measurements. However, the enthalpy of seawater varies nonlinearly with temperature and salinity (Fig. 1) and this variation results in non-conservative behaviour under mixing (McDougall (2003), section A.17 of IOC et al. (2010)). The ocean's potential temperature is subject to internal sources and sinks – it is not conservative.

With the development of a Gibbs function for seawater, based on empirical fits to measurements of known thermodynamic properties (Feistel (2008), IOC et al, 2010), it became possible to apply a more rigorous theory for quasi-equilibrium thermodynamics to study heat content problems in the ocean. As a practical matter, calculations can now be made that allow for an estimate of the magnitude of non-conservative terms in the ocean circulation. By integrating over water depth these production rates can be expressed as an equivalent heat flux per unit area.

Non-conservation of potential temperature was found to be equivalent to a root mean square surface heat flux of about $60\,\mathrm{mW\,m^{-2}}$ (Graham and McDougall, 2013), and an average value of $16\,\mathrm{mW\,m^{-2}}$ (see below). These numbers can be compared to a present-day estimated global-warming surface heat flux imbalance of between $300\,\mathrm{mW\,m^{-2}}$ and $470\,\mathrm{mW\,m^{-2}}$ (Zanna et al., 2019, von Schuckmann et al., 2020). By comparison, the globally averaged rate of increase of temperature due to the dissipation of kinetic energy is equivalent to a surface flux of approximately 10 mW m^{-2}. These equivalent heat fluxes and subsequent similar values are gathered into Table 1 for reference. In the context of a conceptual ocean model being driven by known heat fluxes, the presence of the non-conservation of potential temperature causes SST errors seasonally in the equatorial region of about 0.5K ($0.5°C$), while the error (in all seasons)

155 at the outflow of the Amazon is 1.8K (see section 9 of McDougall, 2003). With different
156 boundary conditions (such as restoring boundary conditions) the error in assuming that
157 potential temperature is conservative is split in different proportions, between (a) the
158 potential temperature values and (b) the potential temperature fluxes.

159 Unfortunately, no single alternative thermodynamic variable has been found that
160 is both independent of pressure, and conservative under mixing. For example, specific
161 entropy is produced in the ocean interior when mixing occurs, with the depth-integrated
162 production being equivalent to an imbalance in the air-sea heat flux of a root mean
163 square value of about $500\,\mathrm{mW\,m^{-2}}$ (Graham and McDougall, 2013), while, apart from the
164 dissipation of kinetic energy, enthalpy is conservative under mixing at constant
165 pressure, but enthalpy is intrinsically pressure-dependent.

166 However, it was found that a constructed variable, potential enthalpy
167 (McDougall, 2003), has a mean non-conservation error in the global ocean of only about
168 $0.3\,\mathrm{mW\,m^{-2}}$ (this is the mean value of an equivalent surface heat flux, equal to the depth
169 integrated interior production of potential enthalpy that is additional to the production
170 due to the dissipation of kinetic energy (Graham and McDougall, 2013)). The potential
171 enthalpy, $\tilde{h}^0$, is the enthalpy of a water parcel after being moved adiabatically and at
172 constant salinity to the reference pressure 0 dbar where the temperature is equal to the
173 potential temperature, θ, of the water parcel:

174 $$\tilde{h}^0\left(S_\mathrm{A},\theta\right) = h\left(S_\mathrm{A},\theta,0\,\mathrm{dbar}\right). \qquad (1)$$

175 In Eq. (1) the function h is the specific enthalpy of TEOS-10 (defined as a function of
176 Absolute Salinity, in-situ temperature and sea pressure) whereas $\tilde{h}^0$ is the potential
177 enthalpy function and the over-twiddle implies that the temperature input to this
178 function is potential temperature, θ. By way of comparison, the area-averaged
179 geothermal input of heat into the ocean bottom is about $86\,\mathrm{mW\,m^{-2}}$, and the interior
180 heating of the ocean due to viscous dissipation, is equivalent to a mean surface heat flux
181 of about $3\,\mathrm{mW\,m^{-2}}$ (Graham and McDougall, 2013). Tailleux (personal communication,
182 2021) has suggested that the dissipation of kinetic energy in the ocean may be as much
183 as three times as large as this value, at approximately 10 mW m^{-2}. Thus we conclude
184 that potential enthalpy, although not a theoretically ideal conservative parameter, can be

185 treated as such for many present purposes in oceanography. If at some stage in the
186 future a source term were to be added to the evolution equation for Conservative
187 Temperature, the most important contribution would be that due to the dissipation of
188 kinetic energy, being a factor of ~10-30 larger than the non-conservation of Conservative
189 Temperature due to other diffusive contributions (namely the terms on the last two lines
190 of Eqn. (38) of Graham and McDougall (2013)).

191 Since potential enthalpy was not a widely understood property, a decision was
192 made in the development of TEOS-10 to adopt Conservative Temperature, Θ, which has
193 units of temperature and is proportional to potential enthalpy:

194 $$\Theta = \tilde{\Theta}\left(S_{\mathrm{A}},\theta\right) = \tilde{h}^{0}\left(S_{\mathrm{A}},\theta\right)\big/ c_{p}^{0}, \qquad (2)$$

195 where the proportionality constant $c_{p}^{0} \equiv 3991.867\,957\,119\,63\ \mathrm{J\,kg^{-1}\,K^{-1}}$, was chosen so that
196 the average value of Conservative Temperature at the ocean surface matched that of
197 potential temperature. Although in hindsight other choices (e.g., with fewer significant
198 digits) might have been more useful, this value of c_{p}^{0} is now built into the TEOS-10
199 standard.

200 Note that at specific locations in the ocean, in particular at low salinities and high
201 temperatures, Θ and θ can differ by more than $1^{\circ}\mathrm{C}$ (Fig. 2); the difference is a strongly
202 nonlinear function of temperature and salinity. Θ is, by definition, independent of
203 adiabatic and isohaline changes in pressure.

204

205 ***Why is potential temperature not conservative?***

206 This question is answered in sections A.17 and A.18 of the TEOS-10 Manual (IOC
207 et al., 2010) as well as McDougall (2003) and Graham and McDougall (2013). The answer
208 is that potential enthalpy referenced to the sea surface pressure, h^{0}, which is an (almost
209 totally) conservative variable in the real ocean, is not simply a linear function of
210 potential temperature, θ, and Absolute Salinity, S_{A} (and note that both enthalpy and
211 entropy are unknown and unknowable up to separate linear functions of Absolute
212 Salinity). If potential enthalpy were a linear function of potential temperature and
213 Absolute Salinity then the "heat content" per unit mass of seawater could be accurately
214 taken to be proportional to potential temperature, and the isobaric specific heat capacity

at zero sea pressure would be a constant. As an example of the nonlinearity of $\tilde{h}^0(S_A,\theta)$, the isobaric specific heat at the sea surface pressure $c_p(S_A,\theta,0\,\mathrm{dbar}) \equiv h^0_\theta$ varies by 6% across the full range of temperatures and salinities found in the World Ocean (Fig. 1). By way of contrast, the potential enthalpy of an ideal gas is proportional to its potential temperature.

Another way of treating heat in an ocean model is to continue carrying potential temperature as its temperature variable but to (i) use the variable isobaric heat capacity at the sea surface to relate the air-sea heat flux to an air-sea flux of potential temperature, and (ii) to evaluate the non-conservative source terms of potential temperature and add these source terms to the potential temperature evolution equation during the ocean model simulation (Tailleux, 2015).

However it is not possible to accurately choose the value of the isobaric heat capacity at the sea surface that is needed when θ is the model's temperature variable. This issue arises because of the unresolved variations in the sea surface salinity (SSS) and SST (for example, unresolved rain events that temporarily lower the SSS), together with the nonlinear dependence of the isobaric specific heat on salinity and temperature. Because of such unresolved correlations, the air-sea heat flux would be systematically mis-estimated. Neither is it possible to accurately estimate the non-conservative source terms of θ in the ocean interior. This problem arises because the source terms are the product of a turbulent flux and a mean gradient. In a mesoscale eddy-resolved ocean model (or even finer scale) it is not clear how to find the eddy flux of θ, as this depends on how the averaging is done in space and time. Furthermore, when analysing the output of such an ocean model, one would need to find a way of dealing with the contributions from source terms that are not expressible in the form of flux convergences when, for example, estimating the meridional heat transport.

We conclude that the idea that ocean models could retain potential temperature θ as the model's temperature variable, rather than adopt the TEOS-10 recommendation of using Conservative Temperature Θ, is unworkable because (1) the air-sea heat flux cannot be accurately evaluated, (2), the non-conservative source terms that appear in the θ evolution equation cannot be estimated accurately, and (3) the ocean section-integrated heat fluxes

cannot be accurately calculated. When contemplating the upgrading ocean model physics, rather than retaining the EOS-80 equation of state and treating the temperature variable as being potential temperature and having to add estimates of the non-conservative production terms to the temperature evolution equation, it is clearly much simpler and more accurate to instead adopt the TEOS-10 equation of state and to treat the model's temperature variable as Conservative Temperature, as recommended by IOC et al. (2010).

How conservative is Conservative Temperature?

This question is addressed in McDougall (2003) as well as in section A.18 of the TEOS-10 Manual (IOC et al., 2010) and in Graham and McDougall (2013). The first step in addressing the non-conservation of Θ is to find a thermophysical variable that is conserved when fluid parcels mix. McDougall (2003) and Graham and McDougall (2013) showed that when fluid parcels are brought together adiabatically and isentropically to mix at pressure p^m, it is the potential enthalpy h^m referenced to the pressure p^m of a mixing event that is conserved, apart from the dissipation of kinetic energy, ε. From this knowledge they constructed the evolution equation for Conservative Temperature (as well as for potential temperature and for entropy).

By contrast, Tailleux (2010) and Tailleux (2015) assumed that it was the Total Energy, being the sum of internal energy, kinetic energy and the geopotential, that is conserved when fluid parcels mix in the ocean. However, as shown by McDougall, Church and Jackett (2003), the $-\nabla\cdot\left(P\mathbf{u}\right)$ term on the right-hand side of the evolution equation for Total Energy is non-zero when integrated over the mixing region, so that Total Energy is not a conservative variable. For a variable to possess the "conservative property", it is not sufficient that the material derivative of that property is given by the divergence of a flux. Rather, what is needed is that the material derivative of a conservative variable must be equal to the divergence of a flux that is zero in the absence of mixing at that location. That is, the flux whose divergence appears on the right-hand side of the evolution equation of a conservative variable must be a diffusive flux (whether a molecular or a turbulent type of diffusive flux). This feature allows one to integrate over a region in which a mixing event is occurring and be confident that there is no flux through the bounding area

that lies outside of the fluid that is being mixed. This is not possible for Total Energy, because even when integrating out to a quiescent surface that encloses an isolated patch of turbulent mixing, the flux divergence term $-\nabla\cdot(P\mathbf{u})$ can still be non-zero there. Note that both contraction-on-mixing and wave processes contribute to $-\nabla\cdot(P\mathbf{u})$.

Tailleux (2010, 2015) treated this non-conservative term, $-\nabla\cdot(P\mathbf{u})$, as though it were a conservative term in all their evolution equations, so that these papers actually arrived at the correct evolution equations for Θ, θ and η (for example, Eqn. (B.7) of Tailleux (2010) and Eqn. (B10) of Graham and McDougall (2013) are identical). However, these equations were written in terms of the molecular fluxes of heat and salt, and the Tailleux (2010, 2015) papers did not find a way to use these expressions to evaluate the non-conservation of Θ, θ and η in a turbulently mixed ocean. This was done in section 3 of Graham and McDougall (2013).

While enthalpy is conserved when mixing occurs at constant pressure, it does not possess the "potential" property, but rather, an adiabatic and isohaline change in pressure causes a change in enthalpy according to $\hat{h}_P = v$, where v is the specific volume. This property is illustrated in Fig. 3 where it is seen that for an adiabatic and isohaline increase of pressure of $1000\,\mathrm{dbar}$, the increase in enthalpy is the same as that caused by an increase in Conservative Temperature of more than $2.4°\mathrm{C}$. If enthalpy variations at constant pressure were a linear function of Absolute Salinity and Conservative Temperature, the contours in Fig. 3 would be parallel equidistant straight lines, and Conservative Temperature would be totally conservative. Since this is not the case, this figure illustrates the (small) non-conservation of Conservative Temperature. Further discussion and evaluation of the non-conservation of Conservative Temperature can be found in McDougall (2003) and Graham and McDougall (2013).

Seawater Salinity

To a degree of approximation which is useful for many purposes, the dissolved matter in seawater ("sea salt") can be treated as a material of uniform composition, whose globally integrated absolute salinity (i.e. the grams of solute per kilogram of seawater) changes only due to the addition and removal of freshwater through rain,

evaporation, and river inflow. This property is because the processes that govern the addition and removal of the constituents of sea salt have extremely long time scales, relative to those that affect the pure water component of seawater. We can thus treat the total ocean salt content as approximately constant, while subject to spatially and temporally varying boundary fluxes of fresh water that give rise to salinity gradients.

The utility of this definition of uniform composition of sea salt lies in its conceptual simplicity, well suited to theoretical and numerical ocean modelling at time scales of up to 100s of years. However, to the demanding degree required for observing and understanding deep ocean pressure gradients, sea salt is neither uniform in composition, nor is it a conserved variable, nor can its absolute amount be measured precisely in practice. The repeatable precision of various technologies used to estimate salinity can be as small as 0.002 g/kg, but the non-ideal nature of seawater means that these estimates can be different by as much as 0.025 g/kg relative to the true Absolute Salinity in the open ocean, and as much 0.1 g/kg in coastal areas (Pawlowicz, 2015).

The most important interior source and sink factors governing changes in the composition of sea salt are biogeochemical processes that govern the biological uptake of dissolved nutrients, calcium, and carbon in the upper ocean, and the remineralization of these substances from sinking particles at depth. At present it is thought that changes resulting from hydrothermal vent activity, fractionation from sea ice formation, and through multi-component molecular diffusion processes are of local importance only, but little work has been done to quantify this.

To address this problem, TEOS-10 defines a Reference Composition of seawater, and several slightly different salinity variables that are necessary for different purposes to account for the variable composition of sea salt. The TEOS-10 Absolute Salinity, S_{A}, is the absolute salinity of Reference Composition Seawater of a measured density (note that capitalization of variable names denotes a precise definition in TEOS-10). It is the salinity variable that is designed to be used to accurately calculate density using the TEOS-10 Gibbs function.

Preformed Salinity, S_*, is the salinity of a seawater parcel with the effects of biogeochemical processes removed, somewhat analogous to a chlorinity-based salinity

335 estimate. It is thus a conservative tracer of seawater, suitable for modelling purposes,
336 but neglects the spatially variable small portion of sea salt involved in biogeochemical
337 processes that is required for the most accurate density estimates. Since the original
338 measurements of specific volume to which both EOS-80 and TEOS-10 were fitted were
339 made on samples of Standard Seawater with composition close to Reference
340 Composition, the Reference Salinity of these samples were also the same as Preformed
341 Salinity.

342 Ocean observational databases contain a completely different variable; Practical
343 Salinity. This variable, which predates TEOS-10, is essentially based on a measure of the
344 electrical conductance of seawater, normalized to conditions of fixed temperature and
345 pressure by empirical correlation equations, between the ranges of 2 and 42 PSS-78 and
346 scaled so that ocean salinity measurements that have been made through a variety of
347 technologies over the past 120 years are numerically comparable. Practical Salinity
348 measurement technologies involve a certified reference material called IAPSO Standard
349 Seawater, which for our purposes can be considered the best available artifact
350 representing seawater of Reference Composition.

351 Practical Salinity was not designed for numerical modelling purposes and does not
352 accurately represent the mass fraction of dissolved matter. We can link Practical
353 Salinity, S_{P}, to the Absolute Salinity of Reference Composition seawater (so-called
354 Reference Salinity, S_{R}) using a fixed scale factor, u_{PS}, so that

355 $$S_{\mathrm{R}} = u_{\mathrm{PS}} S_{\mathrm{P}} \qquad \text{where} \qquad u_{\mathrm{PS}} \equiv (35.165\,04/35)\ \mathrm{g\,kg^{-1}}. \tag{3}$$

356 Conversions to and between the other "salinity" definitions, however, involve
357 knowledge about spatial and temporal variations in seawater composition. Fortunately,
358 the largest component of these changes occurs in a set of constituents involved in
359 biogeochemical processes, whose co-variation is known to be strongly correlated. Thus
360 the Absolute Salinity of real seawater can be determined globally to useful accuracy
361 from the Reference Salinity by the addition of a single parameter, the so-called Absolute
362 Salinity Anomaly, δS_{A},

363 $$S_{\mathrm{A}} = S_{\mathrm{R}} + \delta S_{\mathrm{A}}, \tag{4}$$

364 which has been tabulated in a global atlas for the current ocean (McDougall et al., 2012),
365 and is estimated in coastal areas by considering the effects of river salts (Pawlowicz,
366 2015). It can also be determined from measurements of either density or of carbon and
367 nutrients (IOC et al., 2010, Ji et al., 2021). For purposes of numerical ocean modelling,
368 the Absolute Salinity Anomaly could in theory be obtained by separately tracking the
369 carbon cycle and nutrients, and applying known correction factors, but we are not aware
370 of any attempts to do so.

371 Chemical modelling (Pawlowicz (2010), Wright et al. (2011), Pawlowicz et al.
372 (2012)) suggests the approximate relation

373 $$S_{\mathrm{A}} - S_{*} \approx 1.35\,\delta S_{\mathrm{A}} \equiv 1.35\left(S_{\mathrm{A}} - S_{\mathrm{R}}\right), \tag{5}$$

374 and these relationships are schematically illustrated in Fig. 4. The magnitude of the
375 Absolute Salinity Anomaly is around -.005 to +0.025 g/kg in the open ocean, relative to a
376 mean Absolute Salinity of about 35 g/kg. The correction it implies may be important
377 when initializing models, or comparing them with observations, but its major effect is
378 likely in producing biases in calculated isobaric density gradients.
379
380
381 ***Seawater density***

382 The density of seawater is the most important thermodynamic property affecting
383 oceanic motions, since its spatial changes (along with changes to the sea-surface height)
384 give rise to pressure gradients which are the primary driving force for currents within
385 the ocean interior through the hydrostatic relation. The "traditional" equation of state is
386 known as EOS-80 (UNESCO, 1981), and is standardized as a function of Practical
387 Salinity and in-situ temperature, , $\rho = \rho\left(S_{\mathrm{P}}, t, p\right)$ which has 41 numerical terms. An
388 additional equation (the adiabatic lapse rate) is required for conversion of temperature
389 to potential temperature. However, for ocean models, the EOS-80 equation of state is
390 usually taken to be the 41-term expression written in terms of potential temperature,
391 $\rho = \tilde{\rho}\left(S_{\mathrm{P}}, \theta, p\right)$, of Jackett and McDougall (1995), where the over-twiddle indicates that
392 this rational function fit was made with Practical Salinity S_{P} and potential temperature
393 θ as the input salinity and temperature variables.

394 The current standard for describing the thermodynamic properties of seawater,
395 known as TEOS-10, provides an equation of state, $v = 1/\rho = v(S_A, t, p)$, in the form of a
396 function which involves 72 coefficients (IOC et al., 2010) and is an analytical pressure
397 derivative of the TEOS-10 Gibbs function. However, for ocean models using TEOS-10
398 the equation of state used is one of those in Roquet et al. (2015); the 55-term equation of
399 state, $\rho = \hat{\rho}(S_A, \Theta, z)$, used by Boussinesq models and the 75-term polynomial for specific
400 volume, $v = \hat{v}(S_A, \Theta, p)$, used by non-Boussinesq ocean models.

401 In this paper we will not concentrate on the distinction between Boussinesq and
402 non-Boussinesq ocean models, and henceforth we will take the third input to the
403 equation of state to be pressure, even though for a Boussinesq model it is in fact a scaled
404 version of depth as per the energetic arguments of Young (2010). By the same token, we
405 will cast the discussion in terms of the *in situ* density, even though the non-Boussinesq
406 models have as their equation of state a polynomial for the specific volume, $v = 1/\rho$.

407 For seawater of Reference Composition, both the TEOS-10 and EOS-80 fits
408 $\rho = \hat{\rho}(S_A, \Theta, p)$ and $\rho = \tilde{\rho}(S_P, \theta, p)$ are almost equally accurate (see section A.5 of IOC et
409 al. (2010) and note the comparison between Figures A.5.1 and A.5.2 therein). That is, if
410 we set $\delta S_A = 0$ and use Eqn. (3) to relate Practical and Reference Salinities (which in this
411 case are the same as Preformed Salinities), the numerical density values of in situ density
412 calculated using EOS-80 are not significantly different to those using TEOS-10 in the
413 open ocean [the differences are significant for brackish waters].

414 This being the case, we can see from sections A.5 and A.20 of the TEOS-10
415 Manual (IOC et al. (2010)) that 58% of the data deeper than 1000 dbar in the World
416 Ocean would have the thermal wind misestimated by ~2.7% due to ignoring the
417 difference between Absolute and Reference Salinities. No ocean model has addressed
418 this deficiency to date, but McCarthy et al. (2015) studied the influence of using Absolute
419 Salinity versus Reference Salinity in calculating the overturning circulation in the North
420 Atlantic. They found that the overturning streamfunction changed by 0.7Sv at a depth
421 of 2700m, relative to a mean value at this depth of about 7 Sv, i.e., a 10% effect. Because
422 we argue that the salinity variable in ocean models is best interpreted as being
423 Preformed Salinity, S_*, the neglect of the distinction between Preformed and Absolute

Salinities in ocean models means that they misestimate the overturning streamfunction by 1.35 (see Figure 4) times 0.7Sv, namely ~1Sv, i.e., a 13.5% effect.

Air-sea heat fluxes

Sensible, latent and long-wave radiative fluxes are affected by near-surface turbulence and are usually calculated using bulk formulae involving air and sea surface water temperatures (the air and sea *in situ* temperatures), as well as other parameters (e.g., the latent heat involves the isobaric evaporation enthalpy, commonly called the latent heat of evaporation, which is actually a weak function of temperature and salinity; see Eqn. 6.28 of Feistel et al. (2010) and Eqn. (3.39.7) of IOC et al. (2010)). The total air-sea heat flux, Q, is then translated into a water temperature change by dividing by a heat capacity c_p^0, which has always been taken to be constant in numerical models (Griffies et al., 2016). Although this method is appropriate for Conservative Temperature, CT, (assuming that the TEOS-10 value is used for c_p^0), it is not appropriate when potential temperature is being considered. The flux of potential temperature into the surface of the ocean should be Q divided by $c_p\left(S_*, \theta, 0\right)$. The use of a constant specific heat capacity, in association with the interpretation of the ocean's temperature variable as being potential temperature, means that the ocean has received a different amount of heat than the atmosphere actually delivers to the ocean, and this issue will be explored in section 3.

When precipitation (*P*) occurs at the sea surface, this addition of freshwater brings with it the associated potential enthalpy $h\left(S_{\mathrm{A}}=0,\ t,\ 0\,\mathrm{dbar}\right)$ per unit mass of freshwater, where *t* is the *in situ* temperature of the rain drops as they arrive at the sea surface. The temperature at which rain enters the ocean is not yet treated consistently in coupled models, and section K1.6 of Griffies et al. (2016) suggests that this effect could be equivalent to an area-averaged extra air-sea heat flux of between $-150\ \mathrm{mW\,m^{-2}}$ and $-300\ \mathrm{mW\,m^{-2}}$, representing a heat loss for the ocean.

454 ***Numerical ocean models***

455 In deciding how to numerically model the ocean, an explicit choice must be made
456 about the equation of state, and one would think that this choice would have
457 implications about the precise meaning of the temperature and salinity variables in the
458 model, which we will call T_{model} and S_{model} respectively. We can divide ocean models
459 into two general classes, EOS-80 models, and TEOS-10 models:

460

461 <u>EOS-80 models</u>

462 One class of CMIP ocean model is based around EOS-80, and these models have the
463 following characteristics:

464 1. The model's equation of state, $\rho = \tilde{\rho}\left(S_{\text{P}}, \theta, p\right)$, expects to have Practical Salinity
465 and potential temperature as the salinity and temperature input parameters.
466 2. T_{model} is advected and diffused in the ocean interior in a conservative manner, i.e.,
467 its evolution at a point in space is determined by the convergence of advective
468 fluxes plus parameterized sub-grid scale diffusive and skew diffusive fluxes.
469 3. S_{model} is advected and diffused in the ocean interior in a conservative manner as
470 for T_{model}.
471 4. The air-sea heat flux is delivered to/from the ocean using a constant isobaric
472 specific heat, c_p^0, to convert the air-sea heat flux into a surface flux of T_{model}. [An
473 EOS-80 based model's value of c_p^0 is generally only slightly different to the
474 TEOS-10 value.]
475 5. T_{model} is initialized from an atlas of values of potential temperature, and S_{model} is
476 initialized with values of Practical Salinity.

477 At first glance, it seems reasonable to assume that T_{model} is potential temperature, and
478 S_{model} is Practical Salinity. However, these assumptions imply that theoretical errors
479 arising from items 2 and 3 and 4 are ignored (since neither potential temperature nor
480 Practical Salinity are conservative variables). In this paper we show that these
481 interpretations of the model's temperature and salinity variables are not as accurate as
482 our proposed alternative interpretations.

483

484 TEOS-10 models

485 Other ocean models have begun to implement TEOS-10 features. These models
486 generally have the following characteristics.

487 1. The model's equation of state, $\rho = \hat{\rho}\left(S_{\mathrm{A}}, \Theta, p\right)$, expects to have Absolute Salinity
488 and Conservative Temperature as its salinity and temperature input parameters.
489 2. T_{model} is advected and diffused in the ocean interior in a conservative manner.
490 3. S_{model} is advected and diffused in the ocean interior in a conservative manner.
491 4. At each time step of the model, the value of potential temperature at the sea
492 surface (i.e. SST) is calculated from the T_{model} (which is assumed to be
493 Conservative Temperature) and this value of SST is used to interact with the
494 atmosphere via bulk flux formulae.
495 5. The air-sea heat flux is delivered to/from the ocean using the TEOS-10 constant
496 isobaric specific heat, c_p^0, to convert the air-sea heat flux into a surface flux of
497 T_{model}.
498 6. T_{model} is initialized from an atlas of values of Conservative Temperature, and
499 S_{model} is initialized with values of one of Absolute Salinity, Reference Salinity or
500 Preformed Salinity.

501 Implicitly, it has then been assumed that T_{model} is a Conservative Temperature, and S_{model}
502 is Absolute Salinity.

503 There is one CMIP6 ocean model that we are aware of, ACCESS-CM2 (Australian
504 Community Climate and Earth System Simulator, Bi et al. 2013), whose equation of state
505 is written in terms of Conservative Temperature, but the salinity argument in the
506 equation of state is Practical Salinity. The salinity in this model is initialized with atlas
507 values of Practical Salinity.

508 From the above it is clear that there are small but significant theoretical
509 incompatibilities between different models, and between models and the observed
510 ocean. These issues become apparent when dealing with the technicalities of
511 intercomparisons, and various choices must be made. We now consider the implications
512 of these different choices and provide recommendations for best practices.

513

514 **3. The Interpretation of salinity in ocean models**

515 Note that the samples whose measured specific volumes were incorporated into
516 both the EOS-80 and TEOS-10 equations of state were of Standard Seawater whose
517 composition is close to Reference Composition. Consequently, the EOS-80 and TEOS-10
518 equations of state were constructed with Preformed Salinity, S_* (or, in the case of EOS-
519 80 models, $S_*/u_{\rm PS}$), as their salinity arguments, not Reference Salinity. These same
520 algorithms give accurate values of specific volume for seawater samples that are not of
521 Reference Composition so long as the salinity argument is Absolute Salinity (as opposed
522 to Reference Salinity or Preformed Salinity).

523 For an ocean model that has no non-conservative interior source terms affecting
524 the evolution of its salinity variable, and that is initialized at the sea surface with
525 Preformed Salinity, the only interpretation for the model's salinity variable is Preformed
526 Salinity, and the use of the TEOS-10 equation of state will then yield the correct specific
527 volume. Furthermore, whether the model is initialized with values of Absolute Salinity,
528 Reference Salinity or Preformed Salinity, these initial salinity values are nearly identical
529 in the upper ocean, and any differences between the three initial conditions in the
530 deeper ocean would be largely diffused away within the long spin-up period. That is, in
531 the absence of the non-conservative biogeochemical source terms that would be needed
532 to model Absolute Salinity and to force it away from being conservative (or the smaller
533 source terms that would be needed to maintain Reference Salinity), the model's salinity
534 variable will drift towards being Preformed Salinity. Hence, we conclude that, after the
535 long spin-up phase, the salinity variable of a TEOS-10 based ocean model is accurately
536 interpreted as being Preformed Salinity S_*, irrespective of whether the model was
537 initialized with values of Absolute Salinity, Reference Salinity or Preformed Salinity.

538 Likewise, the prognostic salinity variable after a long spin-up period of an EOS-
539 80 based model is most accurately interpreted as being Preformed Salinity divided by
540 $u_{\rm PS} \equiv (35.165\,04/35)\,{\rm g\,kg^{-1}}$, $S_*/u_{\rm PS}$.

541 We clearly need more estimates of the magnitude of the dynamic effects of the
542 variable seawater composition, but for now we might take a change in 1 Sv in the
543 meridional transport of deep water masses in each ocean basin (based on the Atlantic

work of McCarthy et al., 2015) as an indication of the magnitude of the effect of neglecting the effects of biogeochemistry on salinity. At this stage of model development, since all models are equally deficient in their thermophysical treatment of salinity, at least this aspect does not present a problem as far as making comparisons between CMIP models.

4. Model Heat Flux Calculations

From the details described above, both types of numerical ocean models suffer from some internal contradictions with thermodynamical best practice. For example, for the EOS-80 based models, if $T_{\rm model}$ is assumed to be potential temperature, the use of EOS-80 is correct for density calculations but the use of conservative equations for $T_{\rm model}$ ignores the non-conservative production of potential temperature. The use of a constant heat capacity is also in error if $T_{\rm model}$ is interpreted as potential temperature. Conservative equations are, however, appropriate for Conservative Temperature. In addition, if $S_{\rm model}$ is assumed to be either Practical Salinity or Absolute Salinity, then the use of conservative equations ignores the changes in salinity that arise from biogeochemical processes.

One use for these models is to calculate heat budgets and heat fluxes – both at the surface and between latitudinal bands, and inherent to CMIP is the idea that these different models should be intercompared. The question of how this intercomparison should be done, however, was not clearly addressed in Griffies et al. (2016). Here we begin the discussion by considering two different options for interpreting $T_{\rm model}$ in EOS-80 ocean models.

4.1 Option 1: interpreting the EOS-80 model's temperature as being potential temperature

Under this option the model's temperature variable $T_{\rm model}$ is treated as being potential temperature θ; this is the prevailing interpretation to date. With this interpretation of $T_{\rm model}$ one wonders whether Conservative Temperature Θ should be calculated from the model's (assumed) potential temperature before calculating (i) the global Ocean Heat

574 Content as the volume integral of $\rho c_p^0 \Theta$, and (ii) the advective meridional heat transport
575 as the area integral of $\rho c_p^0 \Theta v$ at constant latitude, where v is the northward velocity.
576 This question was not clearly addressed in Griffies et al. (2016), and here we emphasize
577 one of the main conclusions of the present paper, namely that ocean heat content and
578 meridional heat transports should be calculated using the model's prognostic
579 temperature variable. Any subsequent conversion from one temperature variable to
580 another (such as potential to Conservative) in order to calculate heat content and heat
581 transport is incorrect and confusing, and should not be attempted.
582
583 *4.1.1 Issues with the potential temperature interpretation*
584 There are several thermodynamic inconsistencies that arise from option 1. First,
585 the ocean model has assumed in its spin-up phase (for perhaps a millennium) that T_{model}
586 is conservative, so during the whole spin-up phase and beyond, the contribution of the
587 known non-conservative interior source terms of potential temperature have been
588 absent, and hence the model's temperature variable has not responded to these absent
589 source terms and so this temperature field cannot be potential temperature. Also, since
590 the temperature field of the model is not potential temperature (because of these absent
591 source terms) the velocity field of the model will also not be forced correctly due to
592 errors in the density field which in turn affect the pressure force.
593 The second inconsistent aspect of option 1 is that the air-sea flux of heat is
594 ingested into the ocean model, both during the spin-up stage and during the subsequent
595 transient response phase, as though the model's temperature variable is proportional to
596 potential enthalpy. For example, consider some time during the year at a particular
597 location where the sea surface is fresh (a river outflow, or melted ice). During this time,
598 any heat that the atmosphere loses or gains should have affected the potential
599 temperature of the upper layers of the ocean using a specific heat that is 6% larger than
600 c_p^0 (see Figure 1). So, if the ocean model's temperature variable is interpreted as being
601 potential temperature, a 6% error is made in the heat flux that is exchanged with the
602 atmosphere during these periods/locations. That is, the changes in the ocean model's
603 (assumed) potential temperature caused by the air-sea heat flux will be exaggerated

where and when the sea surface salinity is fresh. This 6% flux error is not corrected by subsequently calculating Conservative Temperature from potential temperature; for example, these temperatures are the same at low temperature and salinity (see Figure 2), and yet at low values of salinity, the specific heat is 6% larger than c_p^0.

This second inconsistent aspect of option 1 can be restated as follows. The adoption of potential temperature as the model's temperature variable means that there is a discontinuity in the heat flux of the coupled air-sea system right at the sea surface; for every Joule of heat (i.e. potential enthalpy) that the atmosphere gives to the ocean, under this Option 1 interpretation, up to 6% too much heat arrives in the ocean over relatively fresh waters. In this way, the adoption of potential temperature as the model temperature variable ensures that the coupled ocean atmosphere system will not conserve heat. Rather, there appear to be non-conservative sources and sinks of heat right at the sea surface where heat is unphysically manufactured or destroyed.

The third inconsistent aspect is a direct consequence of the second; namely that if one is tempted to post-calculate Conservative Temperature Θ from the model's (assumed) values of potential temperature, the rate of change of the calculated ocean heat content as the volume integral of $\rho c_p^0 \Theta$ would no longer be accurately related to the heat that the atmosphere exchanged with the ocean. Neither would the area integral between latitude bands of the air-sea heat flux be exactly equal to the difference between the calculated oceanic meridional heat transports that cross those latitudes. Rather, during the running of the model the heat that was lost from the atmosphere actually shows up in the ocean as the volume integral of the model's prognostic temperature variable. Thus we agree with Appendix D3.3 of Griffies et al. (2016) and strongly recommend that Conservative Temperature is not calculated *a posteriori* in order to evaluate heat content and heat fluxes in these EOS-80 based models.

4.1.2 Quantifying the air-sea flux imbalance

Here we quantify the air-sea flux errors involved with assuming that T_{model} of EOS-80 models is potential temperature. These EOS-80 based models calculate the air-sea flux of their model's temperature as the air-sea heat flux, Q, divided by c_p^0.

634 However, since the isobaric specific heat capacity of seawater at 0 dbar is $c_p(S_*,\theta,0)$, the
635 flux of potential temperature into the surface of the ocean should be Q divided by
636 $c_p(S_*,\theta,0)$. So, if the model's temperature variable is interpreted as being potential
637 temperature, the EOS-80 model has a flux of potential temperature entering the ocean
638 that is too large by the difference between these fluxes, namely by Q/c_p^0 minus
639 $Q/c_p(S_*,\theta,0)$. This means that the ocean has received a different amount of heat than the
640 atmosphere actually delivers to the ocean, with the difference, ΔQ, being $c_p(S_*,\theta,0)$
641 times the difference in the surface fluxes of potential temperature, namely (for the last
642 part of this equation, see Eqn. (A.12.3a) of IOC et al., 2010)

643 $$\Delta Q \;=\; Q\left(\frac{c_p(S_*,\theta,0)}{c_p^0} - 1\right) \;=\; Q\left(\tilde{\Theta}_\theta - 1\right). \qquad (6)$$

644 We plot this quantity from the pre-industrial control run of ACCESS-CM2 in
645 Figure 5c and show it as a cell area-weighted histogram in Figure 5e (note that while
646 these plots apply to EOS-80 based ocean models, to generate these plots we have
647 actually used data from ACCESS-CM2 which is a mostly TEOS-10 compliant model).
648 The calculation takes into account the penetration of shortwave radiation into the ocean
649 but is performed using monthly averages of the thermodynamics quantities. The
650 temperatures and salinities at which the radiative flux divergences occur are taken into
651 account in this calculation. However, the result is little changed if the sea surface
652 temperatures and salinities are used with the radiative flux divergence assumed to take
653 place at the sea surface. Results from similar calculations performed using monthly and
654 daily averaged quantities in ACCESS-OM2 (Kiss et al. 2020) ocean-only model
655 simulations were similar, suggesting that correlations between sub-monthly variations
656 are not significant in such a relatively coarse-resolution model.

657 ΔQ has an area-weighted mean value of $16\,\mathrm{mW\,m^{-2}}$ and we know that this
658 represents the net surface flux of potential temperature required to balance the volume
659 integrated non-conservation of potential temperature in the ocean's interior (Tailleux
660 (2015)). To put this value in context, $16\,\mathrm{mW\,m^{-2}}$ corresponds to 5% of the observed trend
661 of $300\,\mathrm{mW\,m^{-2}}$ in the global ocean heat content from 1955-2017 (Zanna et al. 2019). In
662 addition to this mean value of ΔQ, we see from Figure 5c that there are regions such as

663 the equatorial Pacific and the western north Pacific where ΔQ is as large as the area-
664 averaged heat flux, $300\,\mathrm{mW\,m^{-2}}$, that the ocean has received since 1955. These local
665 anomalies of air-sea flux, if they existed, would drive local variations in temperature.
666 However, these ΔQ values do not represent real heat fluxes. Rather they represent the
667 error in the air-sea heat flux that we make if we insist that the temperature variable in an
668 EOS-80 based ocean model is potential temperature, with the ocean receiving a surface
669 heat flux that is larger by ΔQ than the atmosphere delivers to the ocean. Figure 6 shows
670 the zonal integration of ΔQ, in units of W per degree of latitude.

671 Figure 5e shows that, with T_{model} being interpreted as potential temperature, 5%
672 of the surface area of the ocean needs a surface heat flux that is more than $135\,\mathrm{mW\,m^{-2}}$
673 different to what the atmosphere gives to/from the ocean. This regional variation of ΔQ
674 of approximately $\pm 100\,\mathrm{mW\,m^{-2}}$ is consistent with the regional variations in the air-sea
675 flux of potential temperature found by Graham and McDougall (2013) that is needed to
676 balance the depth-integrated non-conservation of potential temperature as a function of
677 latitude and longitude. This damage that is done to the air-sea heat flux at a given
678 horizontal location by the interpretation that the temperature variable of an EOS-80 ocean
679 model is potential temperature is not small in comparison to the globally averaged rate that
680 our planet is being anthropogenically warmed. That is, in regions that are comparable in
681 size to an ocean basin (see Figure 5(c)), a heat budget analysis using EOS-80 and potential
682 temperature would find a false trend as large as the globally averaged rate that our planet is
683 warming.

684 Figures 5d,f show that much of this spread is due to the variation of the isobaric
685 specific heat capacity on salinity, with the remainder due to the variation of this heat
686 capacity with temperature. We note that if this analysis were performed with a model
687 that resolved individual rain showers and the associated freshwater lenses on the ocean
688 surface, then these episodes of very fresh water at the sea surface would be expected to
689 increase the calculated values of ΔQ. Interestingly, by way of contrast, it is the variation
690 of the isobaric heat capacity with temperature that dominates (by a factor of four) the
691 contribution of this heat capacity variation to the *area-mean* of ΔQ (with the contribution

692 of salinity, ΔQ_S, in Figure. 5d, leading to an area mean of $4\ \mathrm{mW\,m^{-2}}$), as originally found
693 by Tailleux (2015).

694 While a heat flux error of $\pm 100\ \mathrm{mW\,m^{-2}}$ is not large, it also not trivially small, and
695 it seems advisable to respect these fundamental thermodynamic aspects of the coupled
696 Earth system. We will see that this $\pm 100\ \mathrm{mW\,m^{-2}}$ issue is simply avoided by realizing
697 that the temperature variable in these EOS-80 models is not potential temperature.

698 In Appendix A we enquire whether the way that EOS-80 models treat their fluid
699 might be made to be thermodynamically correct for a fluid other than seawater. We find
700 that it is possible to construct such a thermodynamic definition of a fluid with the aim
701 that its treatment in EOS-80 models is consistent with the laws of thermodynamics. This
702 fluid has the same specific volume as seawater for given values of salinity, potential
703 temperature and pressure, but it has different expressions for both enthalpy and
704 entropy. This fluid also has a different adiabatic lapse rate and therefore a different
705 relationship between *in situ* and potential temperatures. However, this exercise in
706 thermodynamic abstraction does not alter the fact that, as a model of the real ocean, and
707 with the temperature variable being interpreted as being potential temperature, the
708 EOS-80 models have ΔQ more heat arriving in the ocean than leaves the atmosphere.

709 Since CMIP6 is centrally concerned with how the planet warms, it is advisable to
710 adopt a framework where heat fluxes and their consequences are respected. That is, we
711 regard it as imperative to avoid non-conservative sources of heat at the sea surface. It is
712 the insistence that the temperature variable in EOS-80 based models is potential
713 temperature that implies that the ocean receives a heat flux from the atmosphere that is
714 larger by ΔQ than what the atmosphere actually exchanges with the ocean. Since there
715 are some areas of the ocean surface where ΔQ is as large as the mean rate of global
716 warming, Option 1 is not supportable. This situation motivates Option 2 where we
717 change the interpretation of the model's temperature variable from being potential
718 temperature to Conservative Temperature even when using EOS-80.

719

720

721 **4.2 Option 2: interpreting the EOS-80 model's temperature as being Conservative**
722 **Temperature**

723 Under this option the ocean model's temperature variable is taken to be Conservative
724 Temperature Θ. The air-sea flux of potential enthalpy is then correctly ingested into the
725 ocean model using the fixed specific heat c_p^0, and the mixing processes in the model
726 correctly conserve Conservative Temperature. Hence the second, fourth and fifth items
727 listed in section 2 are handled correctly, except for the following caveat. In the coupled
728 model, the bulk formulae that set the air-sea heat flux at each time step use the
729 uppermost model temperature as the sea surface temperature as input. So with the
730 Option 2 interpretation of the model's temperature variable as being Conservative
731 Temperature, these bulk formulae are not being fed the SST (which at the sea surface is
732 equal to the potential temperature θ). The difference between these temperatures is
733 $\Theta - \theta$, which is the negative of what we plot in Figure 2. This is a caveat with this
734 Option 2 interpretation, namely that the bulk formula that the model uses to determine
735 the air-sea flux at each time step is a little different to what was intended when the
736 parameters of the bulk formulae were chosen. This is a caveat regarding what was
737 intended by the coupled modeler, rather than what the coupled model experienced.
738 That is, with this Option 2 interpretation, the air-sea heat flux, while being a little bit
739 different than what might have been intended, does arrive in the ocean properly; there is
740 no non-conservative production or destruction of heat at the air-sea boundary as there is
741 in Option 1.

742 Regarding the remaining two items involving temperature listed in section 2, we
743 can dismiss the fifth item, since any small difference in the initial values, set at the
744 beginning of the lengthy spin-up period, between potential temperature and
745 Conservative Temperature will be irrelevant after the long spin-up integration.

746 This then leaves the first point, namely that the model used the equation of state
747 that expects potential temperature as its temperature input, $\tilde{\rho}\left(S_*/u_{\mathrm{PS}}, \theta, p\right)$, but under
748 this Option 2 we are interpreting the model's temperature variable as being
749 Conservative Temperature. In the remainder of this section we address the magnitude
750 of this effect, namely, the use of $\tilde{\rho}\left(S_*/u_{\mathrm{PS}}, \Theta, p\right)$ versus the correct density $\tilde{\rho}\left(S_*/u_{\mathrm{PS}}, \theta, p\right)$

which is almost the same as $\hat{\rho}(S_*,\Theta,p)$. Note, as discussed in section 3 above, the salinity argument of the TEOS-10 equation of state is taken to be S_* while that of the EOS-80 equation of state is taken to be $S_*/u_{\rm PS}$. These salinity variables are simply proportional to each other, and they have the same influence in both equations of state.

Under this Option 2 we are interpreting the model's temperature variable as being Conservative Temperature, and so the density value that the model calculates from its equation of state is deemed to be $\tilde{\rho}(S_*/u_{\rm PS},\Theta,p)$ whereas the density should be evaluated as $\hat{\rho}(S_*,\Theta,p)$ where we remind ourselves that the hat over the *in situ* density function indicates that this is the TEOS-10 equation of state, written with Conservative Temperature as its temperature input. To be clear, under EOS-80 and under TEOS-10 the *in situ* density of seawater of Reference Composition has been expressed by two different expressions,

$$\rho = \tilde{\rho}(S_*/u_{\rm PS},\theta,p) = \hat{\rho}(S_*,\Theta,p), \tag{7}$$

both of which are very good fits to the *in situ* density (hence the equals signs); the increased accuracy of the TEOS-10 equation for density was mostly due to the refinement of the salinity variable, and the increase in the accuracy of TEOS-10 versus EOS-80 for Standard Seawater (Millero et al., 2008) was minor by comparison except for brackish seawater.

We need to ask what error will arise from calculating *in situ* density in the model as $\tilde{\rho}(S_*/u_{\rm PS},\Theta,p)$ instead of as the correct TEOS-10 version of in situ density, $\hat{\rho}(S_*,\Theta,p)$? The effect of this difference on calculations of the buoyancy frequency and even the neutral tangent plane is likely small, so we concentrate on the effect of this difference on the isobaric gradient of *in situ* density (the thermal wind).

Given that under this Option 2 the model's temperature variable is being interpreted as Conservative Temperature, Θ, the model-calculated isobaric gradient of *in situ* density is

$$\tilde{\rho}_{S_*}\nabla_P S_* + \tilde{\rho}_\theta \nabla_P \Theta, \tag{8}$$

whereas the correct isobaric gradient of *in situ* density is actually

$$\hat{\rho}_{S_*}\nabla_P S_* + \hat{\rho}_\Theta \nabla_P \Theta. \tag{9}$$

780 Notice that here and henceforth we drop the scaling factor $u_{\rm PS}$ from the gradient
781 expressions such as Eqn. (8). In any case, this scaling factor cancels from the expression,
782 but we simply drop it for ease of looking at the equations; we can imagine that the EOS-
783 80 equation of state is written in terms of S_* (which would simply require that a first
784 line is added to the computer code which divides the salinity variable by $u_{\rm PS}$).

785 The model's error in evaluating the isobaric gradient of *in situ* density is then the
786 difference between the two equations above, namely

$$\text{787} \qquad \text{error in } \nabla_P \rho \;=\; \left(\tilde{\rho}_{S_*} - \hat{\rho}_{S_*}\right)\nabla_P S_* \;+\; \left(\tilde{\rho}_\theta - \hat{\rho}_\Theta\right)\nabla_P \Theta\,. \tag{10}$$

788 The relative error here in the temperature derivative of the equations of state can be
789 written approximately as

$$\text{790} \qquad \left(\tilde{\rho}_\theta - \hat{\rho}_\Theta\right)\big/\hat{\rho}_\Theta \;=\; \tilde{\alpha}^\theta\big/\hat{\alpha}^\Theta - 1, \tag{11}$$

791 which is the difference from unity of the ratio of the thermal expansion coefficient with
792 respect to potential temperature to that with respect to Conservative Temperature. This
793 ratio, $\tilde{\alpha}^\theta/\hat{\alpha}^\Theta$, can be shown to be equal to $c_p\left(S_*,\theta,0\right)\big/c_p^0$ and we know (from Figure 1)
794 that this varies by 6% in the ocean. This ratio is plotted in Figure 7(a). In regions of the
795 ocean that are very fresh, a relative error in the contribution of the isobaric temperature
796 gradient to the thermal wind will be as large as 6% while in most of the ocean this
797 relative error will be less than 0.5%.

798 Now we turn our attention to the relative error in the salinity derivative of the
799 equation of state, which, from Eqn. (10) can be written approximately as

$$\text{800} \qquad \left(\tilde{\rho}_{S_*} - \hat{\rho}_{S_*}\right)\big/\hat{\rho}_{S_*} \;=\; \tilde{\beta}^\theta\big/\hat{\beta}^\Theta - 1, \tag{12}$$

801 and the ratio, $\tilde{\beta}^\theta/\hat{\beta}^\Theta$, has been plotted (at $p = 0\,\text{dbar}$) in Figure 7(b). This figure shows
802 that the relative error in the salinity derivative, $\left(\tilde{\rho}_{S_*} - \hat{\rho}_{S_*}\right)\big/\hat{\rho}_{S_*}$, is an increasing
803 (approximately quadratic) function of temperature, being approximately zero at $0°\text{C}$, 1%
804 error at $20°\text{C}$ and 2% error at $30°\text{C}$. An alternative derivation of these implications of
805 Eqn. (10) is given in Appendix B.

806 We conclude that under Option 2, where the temperature variable of an EOS-80
807 based model (whose polynomial equation of state expects to have potential temperature
808 as its input temperature) is interpreted as being Conservative Temperature, there are

809 persistent errors in the contribution of the isobaric salinity gradient to the isobaric
810 density gradient that are approximately proportional to temperature squared, with the
811 error being approximately 1% at a temperature of $20°C$ (mostly due to the salinity
812 derivative of *in situ* density at constant potential temperature being 1% different to the
813 corresponding salinity derivative at constant Conservative Temperature). Larger
814 fractional errors in the contribution of the isobaric temperature gradient to the thermal
815 wind equation do occur (of up to 6%) but these are restricted to the rather small volume
816 of the ocean that is quite fresh.

817 In Figure 8 we have evaluated how much the meridional isobaric density
818 gradient changes in the upper 1000 dbar of the World Ocean when the temperature
819 argument in the expression for density is switched from θ to Θ. As explained above,
820 this switch is almost equivalent to the density difference between calling the EOS-80 and
821 the TEOS-10 equations of state, using the same numeric inputs for each. We find that
822 19% of this data has the isobaric density gradient changed by more than 1% when
823 switching from θ to Θ. The median value of the percentage error is 0.22%; that is, 50%
824 of the data shallower than 1000 dbar has the isobaric density gradient changed by more
825 than 0.22% when switching from using EOS-80 to TEOS-10, with the same numerical
826 temperature input, which we are interpreting as being Θ.

827 Figure 8 should not be interpreted as being the extra error involved with taking
828 T_{model} to be Conservative Temperature in EOS-80 ocean models, because, due to the lack
829 of interior non-conservative source terms, the interpretation of T_{model} as being potential
830 temperature is already incorrect by an amount that scales as Θ minus θ. Rather, Figure
831 8 illustrates the error in an EOS-80 model due to the use of an equation of state that is
832 not appropriate to the way that its temperature variable is treated in the model.

833

834 **4.3 Evaluating the options for EOS-80 models**

835 Under option 1 where T_{model} is interpreted as potential temperature, there is a
836 non-conservation of heat at the sea surface, with the ocean seeing one heat flux, and the
837 atmosphere immediately above it seeing another, with 5% of the differences in these

heat fluxes being larger than approximately $\pm 100\,\mathrm{mW\,m^{-2}}$, with a net imbalance of $16\,\mathrm{mW\,m^{-2}}$.

Under option 2 where T_{model} is interpreted as Conservative Temperature, the air-sea flux imbalance does not arise, but two other inaccuracies arise. First, under option 2 the bulk formulae that determine part of the air-sea flux is based on the surface values of Θ rather than of θ (for which the bulk formulae are designed). Second, the isobaric density gradient in the upper ocean is typically different by ~1% to the isobaric density gradient that would be found if the TEOS-10 equation of state had been adopted in these models. These two aspects of option 2 are considered less serious than not conserving heat at the sea surface by up to $\pm 100\,\mathrm{mW\,m^{-2}}$. Neither of the two inaccuracies that arise under option 2 are fundamental thermodynamic errors. Rather they are equivalent to the ocean modeler choosing (i) a slightly different bulk formulae, and (ii) a slightly different equation of state. The constants in the bulk formulae are very poorly known so that the switching from θ to Θ in their use will be well within their uncertainty (Cronin et al., 2019) while the ~1% change to the isobaric density gradient due to using the different equations of state is at the level of our knowledge of the equation of state of sea water (see the discussion section below).

We conclude that option 2 where the T_{model} in EOS-80 models is interpreted as Conservative Temperature is much preferred as it treats the air-sea heat flux in a manner consistent with the First Law of Thermodynamics, and the treatment of T_{model} as being a conservative variable in the ocean interior is more consistent with it being Conservative Temperature than being potential temperature. These same two features of ocean models mean that T_{model} cannot be accurately interpreted as potential temperature, since both the surface flux boundary condition and the lack of the non-conservative source terms in the ocean interior mean that these ocean models continually force T_{model} away from being potential temperature, even if it was initialized as such.

5. Comparison with ocean observations

Now that we have argued that T_{model} of EOS-80 based models should be interpreted as being Conservative Temperature, how then should the model-based

868 estimates of ocean heat content and ocean heat flux be compared with ocean
869 observations and ocean atlas data? The answer is by evaluating the ocean heat content
870 correctly in the observed data sets using TEOS-10, whereby the observed data is used to
871 calculate Conservative Temperature, and this is used together with c_p^0 to evaluate ocean
872 heat content and meridional heat fluxes.

873 We have made the case that the salinity variable in CMIP ocean models that have
874 been spun up for several centuries is Preformed Salinity S_* for the TEOS-10 compliant
875 models, and is $S_*/u_{\rm PS}$ for the EOS-80 compliant models. Hence it is the value of either
876 S_* or $S_*/u_{\rm PS}$ calculated from ocean observations to which the model salinities should be
877 compared. Preformed Salinity S_* is different to Reference Salinity $S_{\rm R}$ by only the ratio
878 $0.26 = 0.35/1.35$ compared with the difference between Absolute Salinity and Preformed
879 Salinity (see Figure 4), and these differences are generally only significantly different to
880 zero at depths exceeding 500 m. Note that Preformed Salinity can be evaluated from
881 observations of Practical Salinity using the Gibbs SeaWater (GSW) software
882 gsw_Sstar_from_SP.
883
884 **6. Discussion and Recommendations**

885 We have made the case that it is advisable to avoid non-conservative sources of
886 heat at the sea surface. It is the prior interpretation of the temperature variable in EOS-
887 80 based models as being potential temperature that implies that the ocean receives a
888 heat flux that is larger by ΔQ than the heat that is lost from the atmosphere. Since there
889 are some areas of the ocean surface where ΔQ is as large as the mean rate of global
890 warming, the issue is important in practice. This realization has motivated the new
891 interpretation of the prognostic temperature of EOS-80 ocean models as being
892 Conservative Temperature (our option 2, section 4.2).

893 A consequence of this new interpretation of the prognostic temperature variable
894 of all CMIP ocean models as being Conservative Temperature means that the EOS-80
895 based models suffer a relative error of ~1% in their isobaric gradient of *in situ* density in
896 the warm upper ocean. How worried should we be about this error? One perspective
897 on this question is to simply note (from above) that there are larger relative errors

898 (~2.7%) in the thermal wind equation in the deep ocean due to the neglect of variations
899 in the relative composition of sea salt. Another perspective is to ask how well science
900 even knows the thermal expansion coefficient, for example. From appendices K and O
901 of IOC et al. (2010) (and section 7 of McDougall and Barker (2011)) we see that the RMS
902 value of the differences between the individual laboratory-based data points of the
903 thermal expansion coefficient and the thermal expansion coefficient obtained from the
904 fitted TEOS-10 Gibbs function is $0.73x10^{-6}$ K^{-1} which is approximately 0.5% of a typical
905 value of the thermal expansion coefficient in the ocean. Without a proper estimation of
906 the number of degrees of freedom represented by the fitted data points, we might
907 estimate the relative error of the thermal expansion coefficient obtained from the fitted
908 TEOS-10 Gibbs function as being half of this, namely 0.25%. So a typical relative error in
909 the isobaric density gradient of ~1% in the upper ocean due to using Θ rather than θ as
910 the temperature input seems undesirable but not serious.

911 We must also acknowledge that all models have ignored the difference between
912 Preformed Salinity, Reference Salinity and Absolute Salinity (which is the salinity
913 variable from which density is accurately calculated). As discussed in IOC et al. (2010),
914 Wright et al. (2011) and McDougall and Barker (2011), glossing over these issues of the
915 spatially variable composition of sea salt, which is the same as glossing over the effects
916 of biogeochemistry on salinity and density, means that all our ocean and climate models
917 have errors in their thermal wind (vertical shear of horizontal velocity) that globally
918 exceed 2.7% for half the ocean volume deeper than 1000 m. In the deep North Pacific
919 Ocean, the misestimation of thermal wind is many times this 2.7% value. The
920 recommended way of incorporating the spatially varying composition of seawater into
921 ocean models appears as section A.20 in the TEOS-10 Manual (IOC et al. (2010), and as
922 section 9 in the McDougall and Barker (2012), with ocean models needing to carry a
923 second salinity type variable. While it is true that this procedure has the effect of
924 relaxing the model towards the non-standard seawater composition of today's ocean, it
925 is clearly advantageous to make a start with this issue by incorporating the non-
926 conservative source terms that apply to the present ocean rather than to continue to
927 ignore the issue altogether. As explained in these references, once the modelling of

928 ocean biogeochemistry matures, the difference between the various types of salinity can
929 be calculated in real time in an ocean model without the need of referring to historical
930 data.

931 Nevertheless, we acknowledge that no published ocean model to date has
932 attempted to include the influence of biogeochemistry on salinity and density, and
933 therefore we recommend that the salinity from both observations and model output be
934 treated as Preformed Salinity S_*.

935

936 ***6.1 Contrasts to the recommendations of Griffies et al. (2016)***

937 How does this paper differ from the recommendations in Griffies et al. (2016)?
938 That paper recommended that the ocean heat content and meridional transport of heat
939 should be calculated using the model's temperature variable and the model's value of
940 c_p^0, and we strenuously agree. However, in the present paper we argue that the
941 temperature variable carried by an EOS-80 based ocean model should be interpreted as
942 being Conservative Temperature, and not be interpreted as being potential temperature.
943 This idea was raised as a possibility in Griffies et al. (2016), but the issue was left unclear
944 in that paper. For example, section D2 of Griffies et al. (2016) recommends that TEOS-10
945 based models archive potential temperature (as well as their model variable,
946 Conservative Temperature) "in order to allow meaningful comparisons" with the output
947 of the EOS-80 based models. We now disagree with this suggestion; the thesis of the
948 present paper is that the temperature variables of both EOS-80 and TEOS-10 based
949 models are already directly comparable, and they should both be interpreted as being
950 Conservative Temperature, and they should both be compared with Conservative
951 Temperature from observations. The fact that the model's temperature variable is
952 labelled "thetao" in EOS-80 models and "bigthetao" in TEOS-10 based models we now
953 see as very likely to cause confusion, since we are recommending that the temperature
954 outputs of both types of ocean models should be interpreted as Conservative
955 Temperature.

956 The present paper also diverges from Griffies et al. (2016) in the way that the
957 salinity variables in CMIP ocean models should be interpreted and thus compared to

observations. Griffies et al. (2016) interpret the salinity variable in TEOS-10 based ocean models as being Reference Salinity S_R whereas we show that these models actually carry Preformed Salinity S_* but have errors in their calculation of densities. Similarly, Griffies et al. (2016) interpret the salinity variable in EOS-80 based ocean models as being Practical Salinity S_P whereas we show that these models actually carry S_*/u_{PS}, that is, Preformed Salinity divided by the constant, u_{PS}. This distinction between the present paper and Griffies et al. (2016) is negligible in the upper ocean where Preformed Salinity is almost identical to Reference Salinity (because the composition of seawater in the upper ocean is close to Reference Composition), but in the deeper parts of the ocean, the distinction is not negligible; for example, based on the work of McCarthy et al. (2015) we have shown that the use of Absolute Salinity versus Preformed Salinity leads to ~1 Sv difference in the meridional overturning streamfunction in the North Atlantic at a depth of 2700 m. However, in this deeper part of the ocean, even though the difference between Absolute Salinity and Preformed Salinity is not negligible, the difference between Preformed Salinity and Reference Salinity (which the TEOS-10 based ocean models have to date assumed their salinity variable to be) is smaller in the ratio 0.35/1.35 = 0.26 (see Figure 4). That is, if the salinity output of a TEOS-10 based ocean model was taken to be Reference Salinity, the error would be only a quarter of the difference between Absolute Salinity and Preformed Salinity, a difference which limits the accuracy of the isobaric density gradients in the deeper parts of ocean models (see Figure 4). A similar remark applies to EOS-80 based ocean models if their salinity output is regarded as being Practical Salinity instead of being (as we propose) S_*/u_{PS}.

6.2 Summary table of ocean heat content imbalances

In Table 1 we summarize the effects of uncertainties in physical or numerical processes in estimating ocean heat content or its changes. The first two rows are the rate of warming (expressed in $\mathrm{mWm^{-2}}$ averaged over the sea surface) due to anthropogenic global warming, and due to geothermal heating. The third row is an estimate of the surface heat flux equivalent of the depth-integrated rate of dissipation of turbulent kinetic energy, and the fourth is an estimate of the neglected net flux of potential

988 enthalpy at the sea surface due to the evaporation and precipitation of water occurring
989 at different temperatures.

990 The next (fifth) row is the consequence of considering the scenario where all the
991 radiant heat is absorbed into the ocean at a pressure of 25 dbar rather than at the sea
992 surface. The derivative of specific enthalpy with respect to Conservative Temperature at
993 25 dbar, $\hat{h}_\Theta$, is c_p^0 times the ratio of the absolute in situ temperature at 25 dbar, $(T_0 + t)$,
994 to the absolute potential temperature, $(T_0 + \theta)$ at this pressure (see Eqn. (A.11.15) of IOC
995 et al. (2010)). The ratio of $\hat{h}_\Theta$ to c_p^0 at 25 dbar is typically different to unity by $6x10^{-6}$,
996 and taking a typical rate of radiative heating of $100\ \mathrm{Wm}^{-2}$ over the ocean's surface leads
997 to $0.6\ \mathrm{mWm}^{-2}$ as the area-averaged rate of mis-estimation of the surface flux of
998 Conservative Temperature for this assumed pressure of penetrative radiation. Since this
999 is so small, the use of c_p^0 (rather than $\hat{h}_\Theta$) to convert the divergence of the radiative heat
1000 flux into a flux of Conservative Temperature is well supported, providing the correct
1001 diagnostics are used for the calculation (such diagnostic issues may be responsible for
1002 the heat budget closure issues identified by Irving et al. 2020).

1003 The next six rows of Table 1 list the mean and twice the standard deviation of the
1004 volume integrated non-conservative production of Conservative Temperature, potential
1005 temperature, and specific entropy, all expressed in mWm^{-2} at the sea surface. The
1006 following two rows are the results we have found in this paper for the air-sea heat flux
1007 error that is made if the EOS-80's temperature is taken to be potential temperature.

1008 The final three rows show that ocean models, being cast in flux divergence form
1009 with heat fluxes being passed between one grid box and the next, do not have
1010 appreciable numerical errors in deducing air-sea fluxes from changes in the volume
1011 integrated heat content.

1012 The estimate from Graham and McDougall (2013) of $-10\ \mathrm{mWm}^{-2}$ is for the net
1013 interior production of θ, so this is a net destruction. A steady state requires this amount
1014 of extra flux of θ at the sea surface (so it can be consumed in the interior). Our estimate
1015 of this extra flux of θ at the sea surface is $16\ \mathrm{mWm}^{-2}$, which is only a little larger than the
1016 estimate of Graham and McDougall (2013).
1017

6.3 Summary of recommendations

In summary, this paper has argued for the following guidelines for analyzing the CMIP model runs. We should

1. interpret the prognostic temperature variable of all CMIP models (whether they are based on the EOS-80 or the TEOS-10 equation of state) as being Conservative Temperature,
2. compare the model's prognostic temperature with the Conservative Temperature, Θ, of observational data,
3. calculate the ocean heat content as the volume integral of the product of (i) in situ density (for non-Boussinesq models or reference density for Boussinesq) (ii) the model's prognostic temperature, Θ, and (iii) the model's value of c_p^0,
4. interpret the salinity variable of the model output as being Preformed Salinity S_* for TEOS-10 based ocean models, and $S_*/u_{\rm PS}$ for EOS-80 based ocean models (so it is advisable to post-multiply the salinity output of EOS-80 models by $u_{\rm PS}$ in order to have the salinity outputs of all types of CMIP models as Preformed Salinity S_*) and,
5. compare the model's salinity variable with Preformed Salinity, S_*, calculated from ocean observations.
6. Sea surface temperature should be taken as the model's prognostic temperature in the case of EOS-80 models (since this is the temperature that was used in the bulk formulae), and as the calculated and stored values of potential temperature in the case of TEOS-10 models.
7. Ensure that all required fixed variables, such as c_p^0, (boussinesq) reference density, seawater volume, and freezing equation are saved to the CMIP archives alongside the prognostic temperature and salinity variables, so that analysts have all components required to accurately interpret the model fields. In addition, providing the full-depth OHC timeseries for each simulation would provide a quantified target for analysts to compare and contrast changes across models and simulations.

Note that this sixth recommendation for EOS-80 based models exposes an unavoidable inconsistency in that the surface values of the model's prognostic temperature is best regarded internally in the ocean model as being Conservative Temperature, but we cannot avoid the fact that this same temperature was used as the sea surface (*in situ*) temperature in the bulk formulae during the running of such ocean models. Issues such as these will not arise when all ocean models have been converted to the TEOS-10 equation of state.

How then should the model's salinity and temperature outputs, S_* and Θ, be used to evaluate dynamical concepts such as streamfunctions, dynamic height, etc? The answer most consistent with the running of a numerical model is to use the equation of state that the model used, together with the model's temperature and salinity outputs on the native grid of the model. This method is important when studying detailed dynamical balances in ocean model output. But since we now have the output salinity and temperature of both EOS-80 and TEOS-10 models being the same (namely S_* and Θ), there is an efficiency and simplicity argument to analyze the output of all these models in the same manner, using algorithms from the Gibbs SeaWater (GSW) Oceanographic Toolbox of TEOS-10 (McDougall and Barker, 2011). Doing these model inter-comparisons often involves interpolating the model outputs to different depths (or pressures) than those used in the original ocean model, so incurring some interpolation errors. While the use of the GSW software means that the *in situ* density will be calculated slightly differently than in some of the forward models, thus affecting the thermal wind and sea-level rise, these differences are small, as can be seen by comparing Figures A.5.1 and A.5.2 of the TEOS-10 Manual, IOC et al. (2010). Hence we think that it is viable for most purposes to evaluate density and dynamic height using the GSW Oceanographic Toolbox, with the input salinity to this GSW code being the model's Preformed Salinity, and the temperature input being the Conservative Temperature, which as we have argued, are the model's prognostic salinity and temperature variables.

Another issue that may arise is where a TEOS-10 based model has been run with Conservative Temperature, but the monthly-mean Conservative Temperature output has been converted into potential temperature before sending the model output to the

CMIP archive. What is the damage done if this inaccurately averaged value of potential temperature is converted back to Conservative Temperature using only the monthly-mean potential temperature and salinity? While such an issue is perhaps an operational detail that takes us some distance from our intention of writing an academic paper about these issues, nevertheless we show Figure 9 which indicates that transforming between these monthly-averaged values is not a serious issue for relatively coarse-resolution ocean models.

Author Contribution

T J McD. devised this new way of interpreting CMIP ocean model variables, P. M. B and R. M. H. provided figures for the paper, and all authors contributed to the concepts and the writing of the manuscript.

Acknowledgements. We have benefitted from comments and suggestions from Drs. Baylor Fox-Kemper, Sjoerd Groeskamp, Casimir de Lavergne, John Krasting, Fabien Roquet, Geoff Stanley, Jan-Erik Tesdal, R. Feistel and R. Tailleux. This paper contributes to the tasks of the Joint SCOR/IAPSO/IAPWS Committee on the Thermophysical Properties of Seawater. T. J. McD., P. M. B. and R. M. H. gratefully acknowledge Australian Research Council support through grant FL150100090. The work of P.J.D. was prepared by Lawrence Livermore National Laboratory (LLNL) under contract no. DE-AC52-07NA27344.

Appendix A: A non-seawater thermodynamic interpretation of Option 1

Ocean models have always assumed a constant isobaric heat capacity and have traditionally assumed that the model's temperature variable is whatever temperature the equation of state was designed to accept. Here we enquire whether there is a way of justifying Option 1 thermodynamically in the sense that Option 1 would be totally consistent with thermodynamic principles for a fluid that is different to real seawater.

That is, we pursue the idea that these EOS-80 based ocean models are not actually models of seawater but are models of a slightly different fluid. We require a fluid that is identical to seawater in some respects, such as that it has the same dissolved material (Millero et al., 2008) and the same issues around Absolute Salinity, Preformed Salinity and Practical Salinity, and the same in situ density as real seawater (at given values of Absolute Salinity, potential temperature and pressure). But we require that the expression for the enthalpy of this new fluid is different to that of real seawater.

The difference that we envisage between real seawater and this new fluid is that, at zero pressure, the enthalpy of the new fluid is given exactly by the constant value c_p^0 times potential temperature θ. That is, for the new fluid, potential enthalpy h^0 is simply $c_p^0\theta$ (as it would be for an ideal gas), and the air-sea interaction for this new fluid would be exactly as it occurs in the EOS-80 based models. Moreover, conservation of potential temperature is justified for this new fluid, and the density and thermal wind would also be correctly evaluated in these EOS-80 based models.

The enthalpy of this new fluid is then given by (since $h_P = v$)

$$\breve{h}\left(S_{\mathrm{A}},\theta,p\right) = c_p^0\,\theta + \int_{P_0}^{P} \tilde{v}\left(S_{\mathrm{A}},\theta,p'\right)\,dP', \tag{A1}$$

while the entropy of this new fluid needs to obey the consistency relationship, $\breve{\eta}_\theta = \breve{h}_\theta\left(p=0\right)/\left(T_0+\theta\right)$, which reduces to

$$\breve{\eta}_\theta = \frac{c_p^0}{\left(T_0+\theta\right)}, \tag{A2}$$

where $T_0 = 273.15\,\mathrm{K}$ is the Celsius zero point. This consistency relationship is derived directly from the Fundamental Thermodynamic Relationship (see Table P.1 of IOC et al.,

2010). Integrating Eqn. (A2) with respect to potential temperature at constant salinity leads to the following expression for entropy that our new fluid must obey,

$$\breve{\eta}\left(S_{\mathrm{A}},\theta\right) = c_p^0 \ln\left(1+\frac{\theta}{T_0}\right) + a\left(\frac{S_{\mathrm{A}}}{S_{\mathrm{SO}}}\right)\ln\left(\frac{S_{\mathrm{A}}}{S_{\mathrm{SO}}}\right). \tag{A3}$$

The variation here with salinity is taken from the TEOS-10 Gibbs-function-derived expression for specific entropy which contains the last term in Eqn. (A3) with the coefficient a being $a = -9.310292413479596\ \mathrm{J\ kg^{-1}\ K^{-1}}$ (this is the value of the coefficient derived from the g_{110} coefficient of the Gibbs function (appendix H of IOC *et al*. (2010)), allowing for our version of the normalization of salinity, $\left(S_{\mathrm{A}}/S_{\mathrm{SO}}\right)$). This term was derived by Feistel (2008) to be theoretically correct at vanishingly small Absolute Salinities.

With these definitions, Eqns. (A1) and (A3), of enthalpy and entropy of our new fluid, we have completely defined all the thermophysical properties of the fluid (see Appendix P of IOC et al., 2010 for a discussion). Many aspects of the fluid are different to seawater, including the adiabatic lapse rate (and hence the relationship between in situ and potential temperatures), since the adiabatic lapse rate is given by $\Gamma = \breve{h}_{\theta P}/\breve{\eta}_\theta$ and while the numerator is the same as for seawater (since $\breve{h}_{\theta P} = \tilde{h}_{\theta P} = \tilde{v}_\theta$), the denominator, $\breve{\eta}_\theta$, which is now given by Eqn. (A2), can be up to 6% different to the corresponding function, $\tilde{\eta}_\theta$, appropriate to real seawater.

We conclude that this is indeed a conceptual way of forcing the EOS-80 based models to be consistent with thermodynamic principles. That is, we have shown that these EOS-80 models are not models of seawater, but they do accurately model a different fluid whose thermodynamic definition we have given in Eqns. (A1) and (A3). This new fluid interacts with the atmosphere in the way that EOS-80 models have assumed to date, the potential temperature of this new fluid is correctly mixed in the ocean in a conservative fashion, and the equation of state is written in terms of the model's temperature variable, namely potential temperature.

Hence we have constructed a fluid which is different thermodynamically to seawater, but it does behave exactly as these EOS-80 models treat their model seawater. That is, we have constructed a new fluid which, if seawater had these thermodynamic

characteristics, then the EOS-80 ocean models would have correct thermodynamics, while being able to interpret the model's temperature variable as being potential temperature.

But this does not change the fact that in order to make these EOS-80 models thermodynamically consistent in this way we have ignored the real variation at the sea surface of the isobaric specific heat capacity; a variation that we know can be as large as 6%.

Hence we do not propose this non-seawater explanation as a useful rationalization of the behaviour of EOS-80 based ocean models. Rather, it seems less dramatic and more climatically relevant to adopt the simpler interpretation of Option 2. Under this option we accept that the model is modelling actual seawater, that the model's temperature variable is in fact Conservative Temperature, and that there are some errors in the equation of state of these EOS-80 models that amount to errors of the order of 1% in the thermal wind relation throughout much of the upper (warm) ocean. That is, so long as we interpret the temperature variable of these EOS-80 based models as Conservative Temperature, they are fine except that they have used an incorrect equation of state; they have used $\tilde{\rho}$ rather than $\hat{\rho}$. Apart from this "error" in the ocean code, Option 2 is a consistent interpretation of the ocean model thermodynamics and dynamics. In ocean models there are always questions of how to parameterize ocean mixing. To this uncertain aspect of ocean physics, under Option 2 we add the less than desirable expression that is used to evaluate density in EOS-80 based ocean models in CMIP

Appendix B: An alternative derivation of Eqn. (10)

Eqn. (10) is an expression for the error in the isobaric density gradient when Conservative Temperature is used as the input temperature variable to the EOS-80 equation of state (which expects its input temperature to be potential temperature). An alternative accurate expression to Eqn. (9) for the isobaric density gradient is

$$\tilde{\rho}_{S_*} \nabla_P S_* + \tilde{\rho}_\theta \nabla_P \theta \,, \tag{B1}$$

and subtracting this from the incorrect expression, Eqn. (8), gives the following expression for the model's error in evaluating the isobaric gradient of in situ density,

$$\text{error in } \nabla_P \rho \;=\; \tilde{\rho}_\theta \, \nabla_P \left(\Theta - \theta \right). \tag{B2}$$

An approximate fit to the temperature difference, $\Theta - \theta$, as displayed in Figure 2 is

$$\left(\Theta - \theta \right) \approx 0.05 \, \Theta \left(1 - \frac{S_{\rm A}}{S_{\rm SO}} \right) - 1.75 x 10^{-3} \Theta \left(1 - \frac{\Theta}{25^\circ{\rm C}} \right), \tag{B3}$$

and using this approximate expression in the right-hand side of Eqn. (B2) gives

$$\frac{\text{error in } \nabla_P \rho}{\tilde{\rho}_\theta} \approx \left[0.05 \left(1 - \frac{S_*}{S_{\rm SO}} \right) - 1.75 x 10^{-3} \left(1 - \frac{\Theta}{12.5^\circ{\rm C}} \right) \right] \nabla_P \Theta \;-\; \frac{0.05}{S_{\rm SO}} \, \Theta \, \nabla_P S_* \,. \tag{B4}$$

The first part of this expression that multiplies $\nabla_P \Theta$ corresponds to the proportional error in the thermal expansion coefficient displayed in Figure 7(a). The second part of Eqn. (B4) amounts to an error in the saline derivative of the equation of state, with the proportional error (corresponding to Eqn. (12)), being $-0.05 \tilde{\rho}_\theta \Theta \Big/ \left(\hat{\rho}_{S_{\rm A}} S_{\rm SO} \right)$, and this is close to the error that can be seen in Figure 7(b). This error is approximately a quadratic function of temperature since the thermal expansion coefficient $\tilde{\rho}_\theta$ is approximately a linear function of temperature.

	Heat flux contributions of different processes	mWm^{-2}
Physical processes	Global warming imbalance (Zanna et al., 2019), mean	**+300**
	Geothermal heating (Emile-Geay and Madec, 2009), mean	**+86**
	Viscous dissipation (Graham and McDougall, 2013), mean	**+3**
	Atmospheric water fluxes of enthalpy (Griffies et al. 2016), mean	**- (150-300)**
Non-conservation errors	Extra flux of Θ if the air-sea radiative heat flux is taken to occur at a pressure of 25dbar	**-0.6**
	non-conservation of Θ (Graham & McDougall 2013), mean	**+0.3**
	non-conservation of Θ (Graham & McDougall 2013), 2*rms	**+1**
	non-conservation of θ (Graham & McDougall 2013), mean	**-10**
	non-conservation of θ (Graham & McDougall 2013), 2*rms	$\pm$**120**
	non-conservation of η (Graham & McDougall 2013), mean	**+380**
	non-conservation of η (Graham & McDougall 2013), 2*rms	**+1200**
	Interpreting EOS-80 T as θ (ACCESS-CM2 estimate), mean	**+16**
	Interpreting EOS-80 T as θ (ACCESS-CM2 estimate), 2*rms	$\pm$**135**
Numerical errors	ACCESS-OM2 single time-step	$\pm$**10^(-7)**
	ACCESS-OM2 diagnosed from OHC snapshots	$\pm$**0.001**
	ACCESS-CM2 diagnosed from OHC monthly-averages	$\pm$**0.03**

Table 1: Summary of the impact of various processes and modelling errors on the global ocean heat budget and its imbalance. All numbers are in units of mWm^{-2}. Numerical errors are diagnosed from either ACCESS-OM2 (machine precision errors) or ACCESS-CM2 (associated with not having access to OHC snapshots). Numbers from interior processes are converted to equivalent surface fluxes by depth integration. The sign convention here is that a positive heat flux is heat entering the ocean or warming the ocean by internal dissipation. The symbol η in this table stands for entropy.

Code Availability

This paper has not run any ocean or climate models, and so has not produced any such computer code. Processed data and code to produce the ACCESS-CM2 figures 5, 6 and 9 is located at the github repository https://github.com/rmholmes/ACCESS_CM2_SpecificHeat.

Data Availability

This paper has not produced any model data. Processed data and code to produce the ACCESS-CM2 figures 5, 6 and 9 is located at the github repository https://github.com/rmholmes/ACCESS_CM2_SpecificHeat.

References

Bi, D., Dix, M., Marsland, S., O'Farrell, S., Rashid, H., Uotila, P., Hirst, A., Kowalczyk, E., Golebiewski, M., Sullivan, A., Yan, H., Hannah, N., Franklin, C., Sun, Z., Vohralik, P., Watterson, I., Zhou, X., Fiedler, R., Collier, M., Ma, Y., Noonan, J., Stevens, L., Uhe, P., Zhu, H., Griffies, S., Hill, R., Harris, C. and Puri, K.: The ACCESS coupled model: description, control climate and evaluation, *Aust. Met. Oceanogr. J.*, **63**, 41-64, 2013.

Cronin M. F., Gentemann C. L., Edson J., Ueki I., Bourassa M., Brown S., Clayson C. A., Fairall C. W., Farrar J. T., Gille S. T., Gulev S., Josey S. A., Kato S., Katsumata M., Kent E., Krug M., Minnett P. J., Parfitt R., Pinker R. T., Stackhouse P. W., Swart S., Tomita H., Vandemark D., Weller A. R., Yoneyama K., Yu L., Zhang D.: Air-Sea Fluxes With a Focus on Heat and Momentum. *Frontiers in Marine Science*, **6**, 430. https://www.frontiersin.org/article/10.3389/fmars.2019.00430 , 2019.

Emile-Geay J. and Madec G.: Geothermal heating, diapycnal mixing and abyssal circulation. *Ocean Science*, **5**, 203-217, 2019.

Feistel, R.: A Gibbs function for seawater thermodynamics for −6 to 80 °C and salinity up to 120 g kg^{-1}, *Deep-Sea Res. I*, **55**, 1639-1671, 2008.

Feistel, R., Wright D. G., Kretzschmar H.-J., Hagen E., Herrmann S. and Span R.: Thermodynamic properties of sea air. *Ocean Science,* **6**, 91–141. http://www.ocean-sci.net/6/91/2010/os-6-91-2010.pdf , 2010.

Graham, F. S. and McDougall T. J.: Quantifying the non-conservative production of Conservative Temperature, potential temperature and entropy. *Journal of Physical Oceanography*, **43**, 838-862. http://dx.doi.org/10.1175/JPO-D-11-0188.1 , 2013.

Griffies, S. M., Danabasoglu, G., Durack, P. J., Adcroft, A. J., Balaji, V., Böning, C. W., Chassignet, E. P., Curchitser, E., Deshayes, J., Drange, H., Fox-Kemper, B., Gleckler, P. J., Gregory, J. M., Haak, H., Hallberg, R. W., Heimbach, P., Hewitt, H. T., Holland, D. M., Ilyina, T., Jungclaus, J. H., Komuro, Y., Krasting, J. P., Large, W. G., Marsland, S. J., Masina, S., McDougall, T. J., Nurser, A. J. G., Orr, J. C., Pirani, A., Qiao, F., Stouffer, R. J., Taylor, K. E., Treguier, A. M., Tsujino, H., Uotila, P., Valdivieso, M., Wang, Q., Winton, M., and Yeager, S. G.: OMIP contribution to CMIP6: experimental and diagnostic protocol for the physical component of the Ocean Model Intercomparison

Project: *Geosci. Model Dev.*, **9**, 3231-3296, doi:10.5194/gmd-9-3231-2016. http://dx.doi.org/10.5194/gmd-9-3231-2016 , 2016.

IOC, SCOR and IAPSO: *The international thermodynamic equation of seawater – 2010: Calculation and use of thermodynamic properties*. Intergovernmental Oceanographic Commission, Manuals and Guides No. 56, UNESCO (English), 196 pp. available at http://www.TEOS-10.org/pubs/TEOS-10_Manual.pdf Many of the original papers on which TEOS-10 is based were published in the following Special Issue of *Ocean Science*, https://os.copernicus.org/articles/special_issue14.html 2010.

Irving, D., Hobbs W., Church J. and Zika J.: A Mass and Energy Conservation Analysis of Drift in the CMIP6 Ensemble. *Journal of Climate*, **34**, 3157-3170, https://doi.org/10.1175/JCLI-D-20-0281.1, 2021.

Jackett, D. R. and McDougall T. J.: Minimal adjustment of hydrographic profiles to achieve static stability. *Journal of Atmospheric and Oceanic Technology*, **12**, 381-389. https://journals.ametsoc.org/doi/abs/10.1175/1520-0426%281995%29012%3C0381%3AMAOHPT%3E2.0.CO%3B2 , 1995.

Ji, F., Pawlowicz, R., Xiong, X.: Estimating the Absolute Salinity of Chinese offshore waters using nutrients and inorganic carbon data. *Ocean Sci.*, **17**, 909–918, https://doi.org/10.5194/os-17-909-2021, 2021.

McCarthy, G.D., Smeed, D.A., Johns, W.E., Frajka-Williams, E., Moat, B.I., Rayner, D., Baringer, M.O., Meinen, C.S., Collins, J. and Bryden, H.L.: Measuring the Atlantic Meridional Overturning Circulation at 26°N. *Progress in Oceanography*, **130**, 91-111. doi:10.1016/j.pocean.2014.10.006 , 2015.

McDougall, T. J.: Potential enthalpy: A conservative oceanic variable for evaluating heat content and heat fluxes. *Journal of Physical Oceanography*, **33**, 945-963. https://journals.ametsoc.org/jpo/article/33/5/945/10023/ , 2003.

McDougall T. J. and Barker P. M.: *Getting started with TEOS-10 and the Gibbs Seawater (GSW) Oceanographic Toolbox*, 28pp, SCOR/IAPSO WG127, ISBN 978-0-646-55621-5. available at http://www.TEOS-10.org/pubs/Getting_Started.pdf , 2011.

1287 McDougall, T. J., Church J. A. and Jackett, D. R.: Does the nonlinearity of the equation
1288 of state impose an upper bound on the buoyancy frequency? *Journal of Marine*
1289 *Research*, **61**, 745-764, http://dx.doi.org/10.1357/002224003322981138 , 2003.
1290 McDougall, T. J. and Feistel R.: What causes the adiabatic lapse rate? *Deep-Sea Research I,*
1291 **50**, 1523-1535. http://dx.doi.org/10.1016/j.dsr.2003.09.007 , 2003.
1292 McDougall, T. J., Jackett D. R., Millero F. J., Pawlowicz R. and Barker P. M.: A global
1293 algorithm for estimating Absolute Salinity. *Ocean Science*, **8**, 1123-1134.
1294 http://www.ocean-sci.net/8/1123/2012/os-8-1123-2012.pdf , 2012.
1295 Millero, F. J., Feistel R., Wright D. G. and McDougall T. J.: The composition of Standard
1296 Seawater and the definition of the Reference-Composition Salinity Scale. *Deep-Sea*
1297 *Research-I*, **55**, 50-72. http://dx.doi.org/10.1016/j.dsr.2007.10.001 , 2008.
1298 Pawlowicz, R.: A model for predicting changes in the electrical conductivity, Practical Salinity,
1299 and Absolute Salinity of seawater due to variations in relative chemical composition. *Ocean*
1300 *Science,* **6**, 361–378. http://www.ocean-sci.net/6/361/2010/os-6-361-2010.pdf , 2010.
1301 Pawlowicz, R.: The Absolute Salinity of seawater diluted by riverwater. *Deep-Sea Research I*,
1302 **101**, 71-79, 2015.
1303 Pawlowicz, R., Wright D. G. and Millero F. J.: The effects of biogeochemical processes on
1304 oceanic conductivity/salinity/density relationships and the characterization of real seawater.
1305 *Ocean Science,* **7**, 363–387. http://www.ocean-sci.net/7/363/2011/os-7-363-2011.pdf, 2011.
1306 Pawlowicz, R., McDougall T., Feistel R. and Tailleux R.: An historical perspective on the
1307 development of the Thermodynamic Equation of Seawater – 2010: *Ocean Sci.*, **8**, 161-
1308 174. http://www.ocean-sci.net/8/161/2012/os-8-161-2012.pdf , 2012.
1309 Roquet, F., Madec G., McDougall T. J. and Barker P. M.: Accurate polynomial expressions for
1310 the density and specific volume of seawater using the TEOS-10 standard. *Ocean*
1311 *Modelling*, **90**, 29-43. http://dx.doi.org/10.1016/j.ocemod.2015.04.002 , 2015.
1312 Tailleux, R.: Identifying and quantifying nonconservative energy production/destruction terms
1313 in hydrostatic Boussinesq primitive equation models. *Ocean Modelling*, **34**, 125-136,
1314 https://doi.org/10.1016/j.ocemod.2010.05.003 , 2010.

1315 Tailleux, R.: Observational and energetics constraints on the non-conservation of
1316 potential/Conservative Temperature and implications for ocean modelling. *Ocean*
1317 *Modelling*, **88**, 26-37. https://doi.org/10.1016/j.ocemod.2015.02.001 , 2015.
1318 von Schuckmann, K. et al. Heat stored in the Earth system: where does the energy go? *Earth*
1319 *Syst. Sci. Data*, **12**, 2013-2041, 2020.
1320 Wright, D. G., Pawlowicz R., McDougall T. J., Feistel R. and Marion G. M.: Absolute Salinity,
1321 "Density Salinity" and the Reference-Composition Salinity Scale: present and future use
1322 in the seawater standard TEOS-10. *Ocean Sci.*, **7**, 1-26. http://www.ocean-
1323 sci.net/7/1/2011/os-7-1-2011.pdf , 2011.
1324 Young, W.R., Dynamic Enthalpy, Conservative Temperature, and the Seawater Boussinesq
1325 Approximation, *Journal of Physical Oceanography*, **40**, 394-400,
1326 doi: 10.1175/2009JPO4294.1 , 2010.
1327 Zanna L., Khatiwala S., Gregory J. M., Ison, J. and Heimbach P.: Global reconstruction of
1328 historical ocean heat storage and transport, *Proceedings of the National Academy of*
1329 *Sciences*, **116**, 1126-1131, 2019.

1330
1331

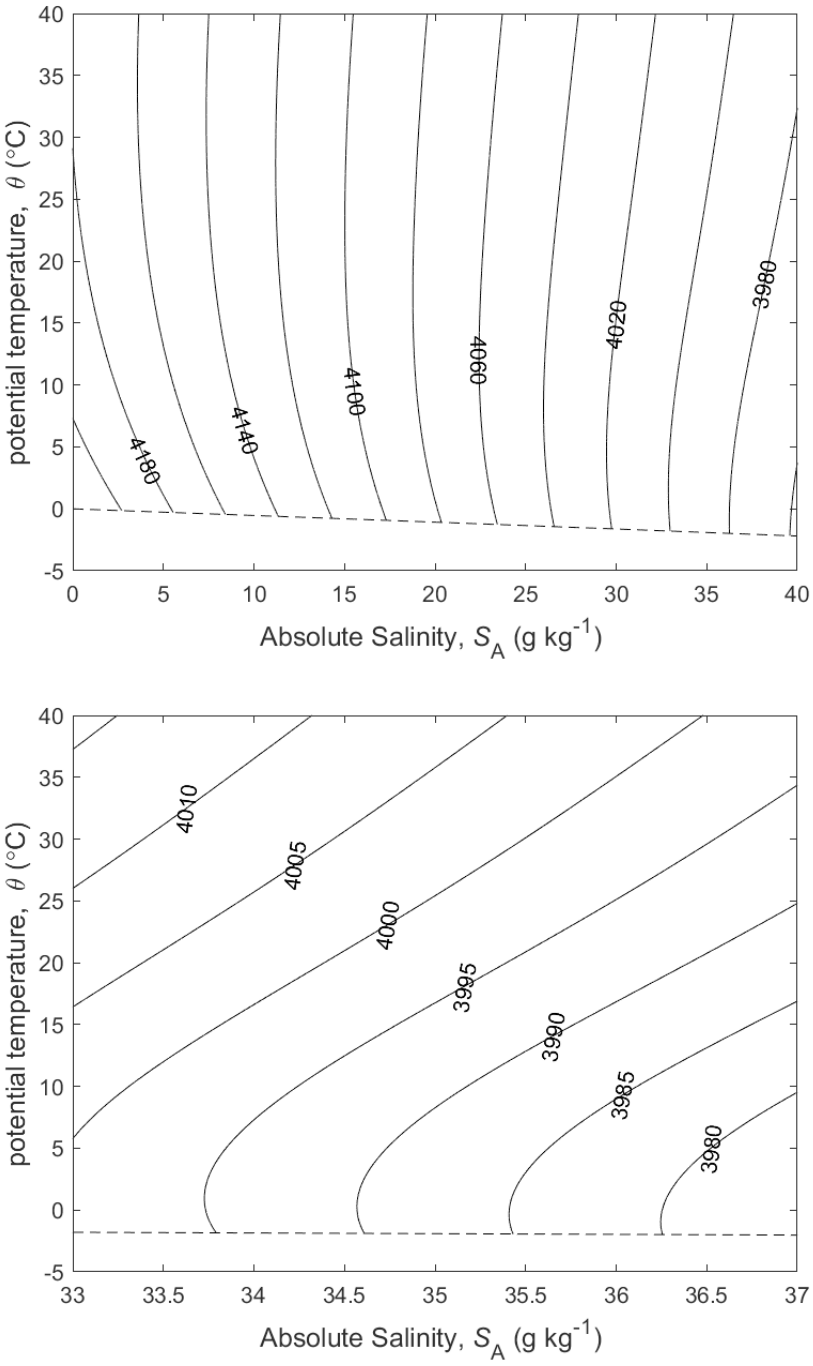

Figure 1. (a) Contours of isobaric specific heat capacity c_p of seawater (in J kg^{-1} K^{-1}), at $p = 0$ dbar. (b) a zoomed-in version for a smaller range of Absolute Salinity. The dashed line is the freezing line at $p = 0$ dbar.

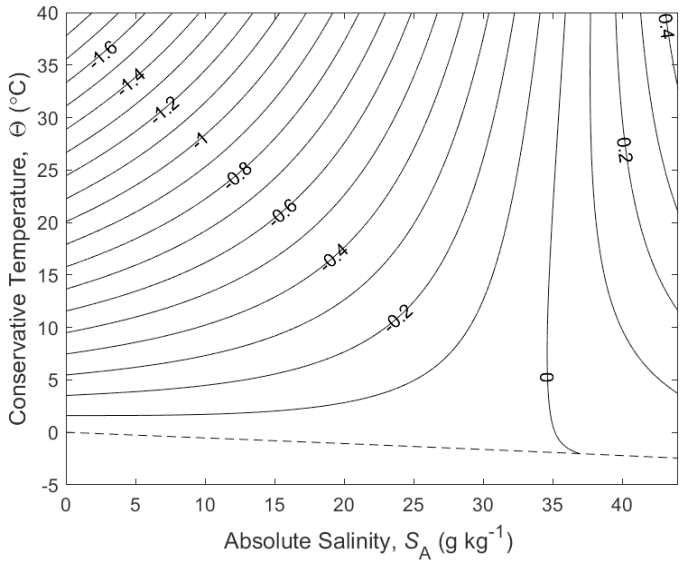

Figure 2. Contours (in °C) of the difference between potential temperature and Conservative Temperature, $\theta - \Theta$.

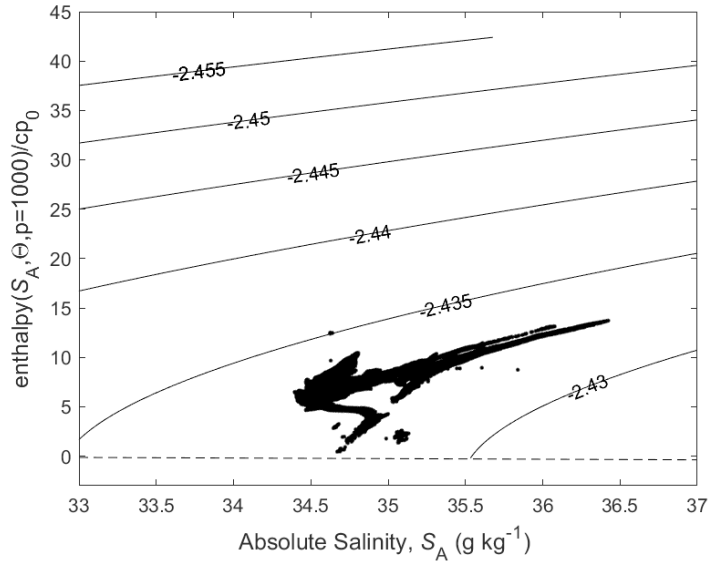

Figure 3. Contours of $\Theta - \hat{h}\left(S_A, \Theta, 1000\,\text{dbar}\right)/c_p^0$ on the Absolute Salinity – $\hat{h}\left(S_A, \Theta, 1000\,\text{dbar}\right)/c_p^0$ diagram. Enthalpy, $\hat{h}\left(S_A, \Theta, 1000\,\text{dbar}\right)$, is a conservative quantity for turbulent mixing processes that occur at a pressure of 1000 dbar. The mean value of the contoured quantity is approximately -2.44°C illustrating that enthalpy does not possess the "potential" property; that is, enthalpy increases during adiabatic and isohaline increases in pressure. The fact that the contoured quantity on this figure is not a linear function of S_A and $\hat{h}\left(S_A, \Theta, 1000\,\text{dbar}\right)$ illustrates the (small) non-conservative nature of Conservative Temperature. The dots are data from the word ocean at 1000 dbar.

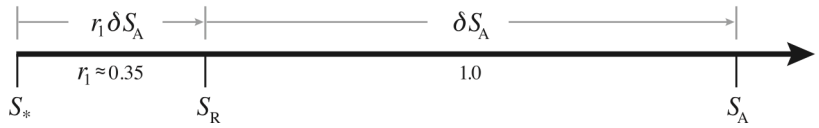

Figure 4. Number line of salinity, illustrating the differences between Preformed Salinity S_*, Reference Salinity S_R, and Absolute Salinity S_A for seawater whose composition differs from that of Standard Seawater which has Reference Composition. If a seawater sample has Reference Composition, then $\delta S_A = 0$ and S_*, S_R and S_A are all equal.

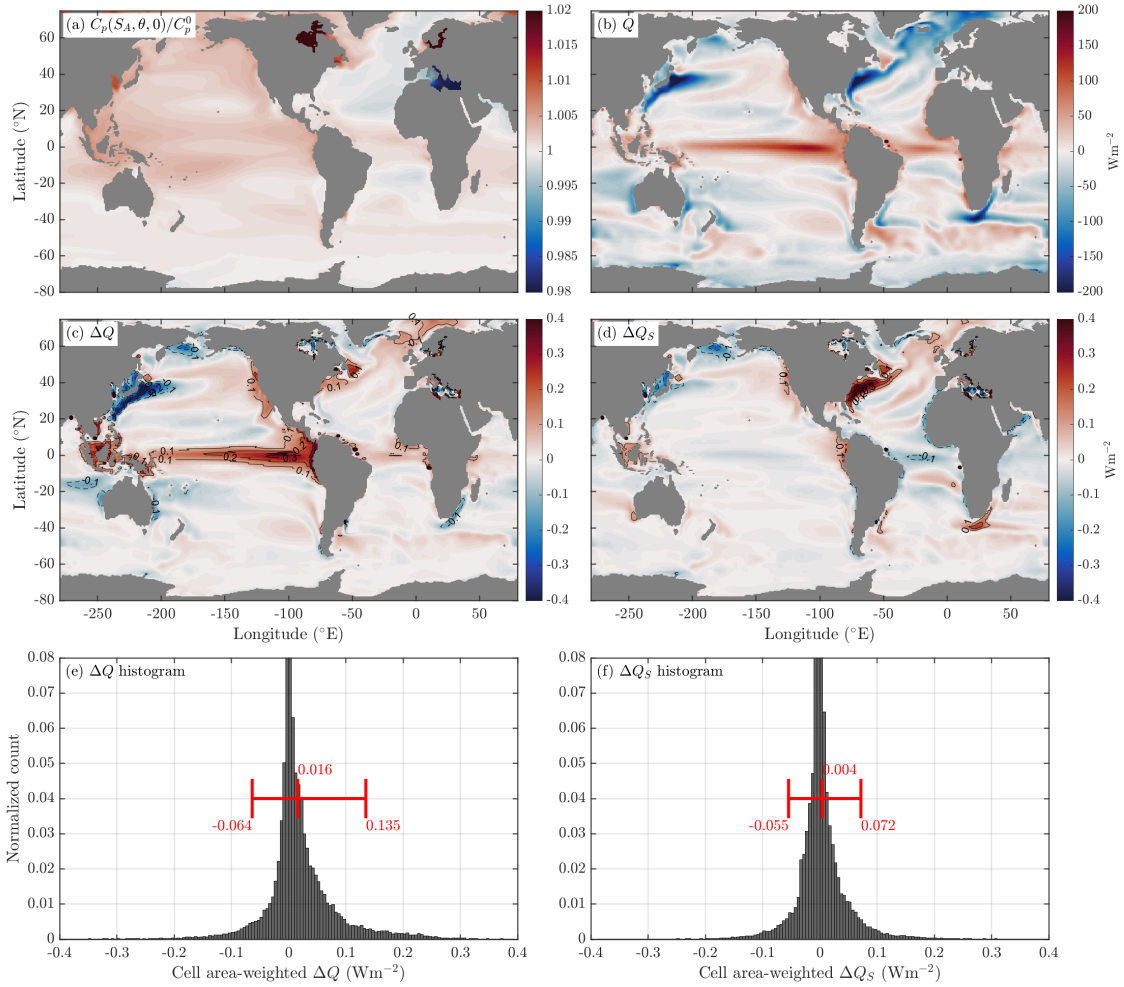

Figure 5. (a) The average value of the ratio of the isobaric specific heat of seawater and c_p^0 for data from the ACCESS-CM2 model's pre-industrial control simulation (600 years long). (b) The average surface heat flux Q (Wm^{-2}) in this same ocean model. (c) The additional heat that the ocean receives/loses compared to the heat that the atmosphere loses/receives (assuming that an EOS-80 model's temperature variable is potential temperature), ΔQ ($\mathrm{W\,m^{-2}}$, Eqn. 6). (e) a histogram of ΔQ weighted by the area of each grid cell. (d) The contribution of salinity variations to the air-sea heat flux discrepancy, given by $\Delta Q_S = Q\left(S-\overline{S}\right)\left(1/c_p^0\right)\partial c_p/\partial S$, where $\overline{S}$ is the surface mean salinity and $\partial c_p/\partial S$ is the variation in the specific heat with salinity at the surface mean salinity and potential temperature. (f) a histogram of ΔQ_S weighted by the area of each grid cell. Shown in red in panels e and f are the mean, 5$^{\text{th}}$ and 95$^{\text{th}}$ percentiles of the histogram ($\mathrm{W\,m^{-2}}$). Note that these calculations neglect correlations between surface properties and the surface heat flux at sub-monthly time scales.

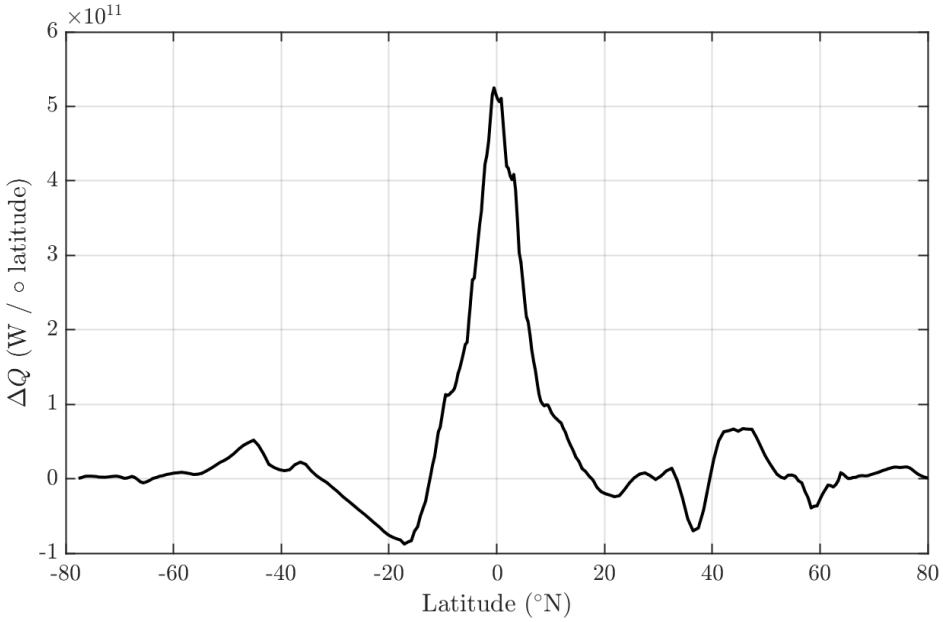

Figure 6. The ACCESS-CM2 zonally integrated ΔQ From Fig.5c, showing the imbalance in the air-sea heat flux in Watts per degree of latitude.

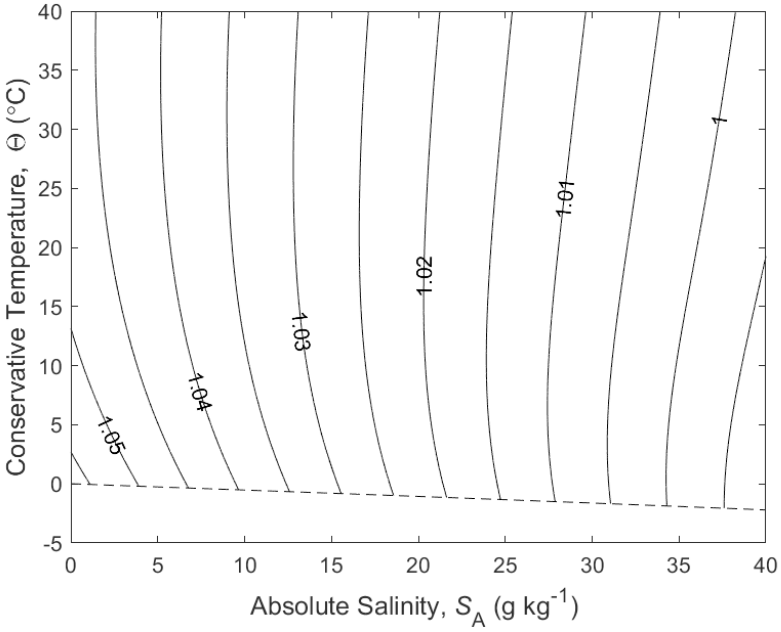

1395

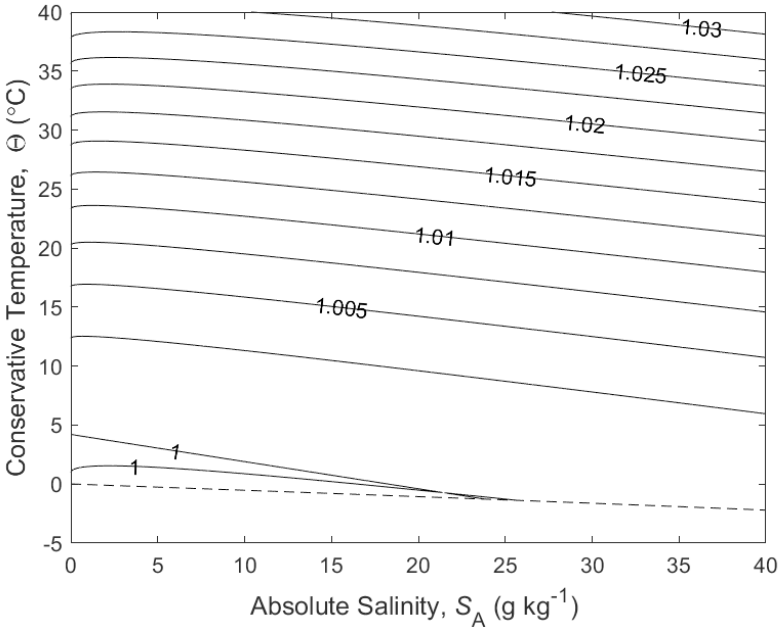

1396
1397

1398 **Figure 7.** (a) The ratio of the thermal expansion coefficients with respect to Conservative
1399 Temperature and potential temperature, $\tilde{\alpha}^\theta / \hat{\alpha}^\Theta = \tilde{\Theta}_\theta$. (b) The ratio of the saline
1400 contraction coefficients at constant potential temperature to that at constant Conservative
1401 Temperature, $\tilde{\beta}^\theta / \hat{\beta}^\Theta = 1 + \left(\hat{\alpha}^\Theta / \hat{\beta}^\Theta\right) \hat{\theta}_{S_A} / \hat{\theta}_\Theta$ at $p = 0$ dbar.

1402

1403

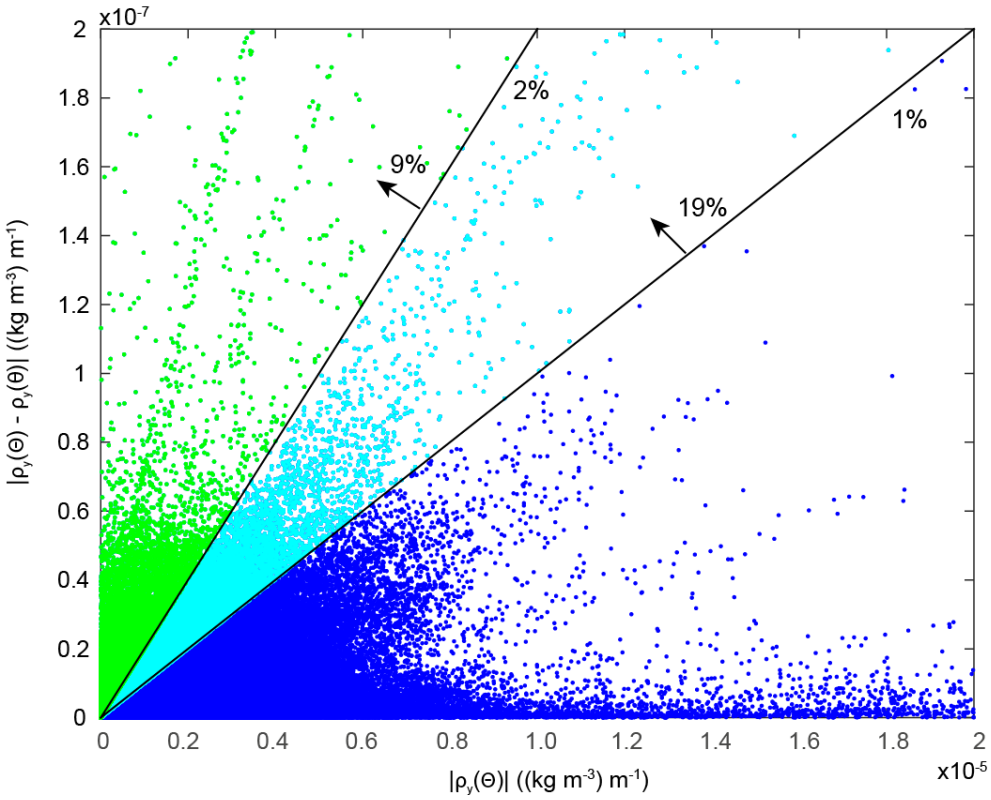

Figure 8. The northward density gradient at constant pressure (the horizontal axis) for data in the global ocean atlas of Gouretski and Koltermann (2004) for $p < 1000$ dbar. The vertical axis is the magnitude of the difference between evaluating the density gradient using Θ versus θ as the temperature argument in the expression for density. This is virtually equivalent to the density difference between calling the EOS-80 and the TEOS-10 equations of state, using the same numeric inputs for each. The 1% and 2% lines indicate where the isobaric density gradient is in error by 1% and 2%. 19% of the data shallower than 1000 dbar has the isobaric density gradient changed by more than 1% when switching between the equations of state. The median value of the percentage error in the isobaric density gradient is 0.22%.

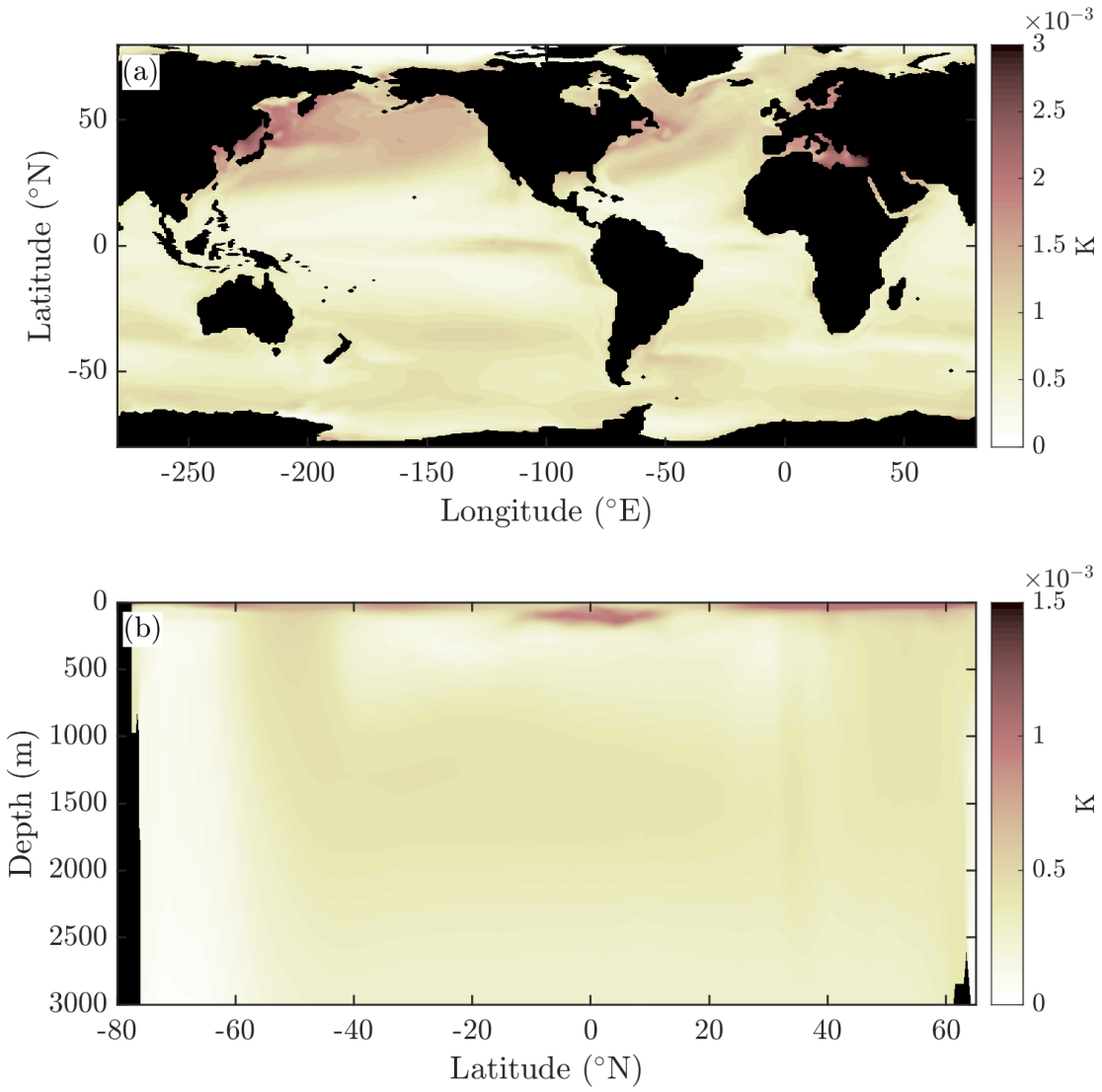

Figure 9. The RMS error (K) in evaluating Conservative Temperature from the CMIP6 archived monthly-averaged values of potential temperature and salinity, compared with averaging the instantaneous values of Conservative Temperature for a month at the (a) surface and (b) the zonal mean. These quantities are calculated from 50 years of temporally averaged output from the ACCESS-CM2 model's pre-industrial control simulation. The errors are seen to be no larger than a few mK.